International Journal of Environmental Epidemiology

OPEN ACCESS
Article

PFOA impairs angiogenesis via PKA/GSK-3β/β-catenin/Snail signaling, revealing a novel mechanism for cardiotoxicity

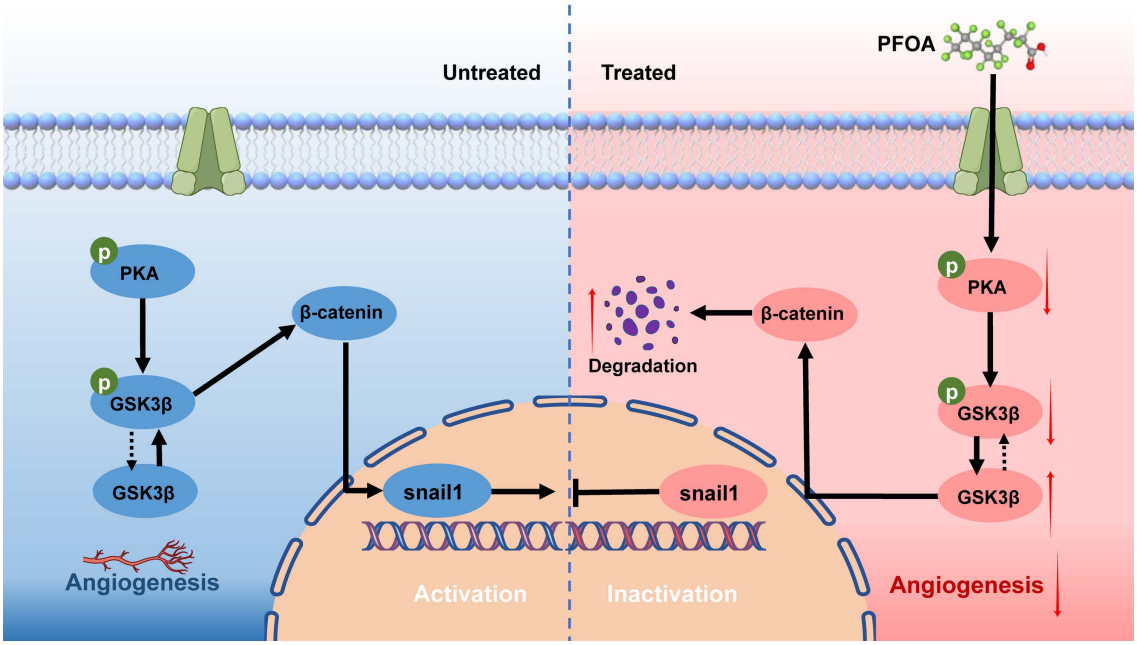
He Xiao, Yixuan Liu, Lujiao Yu, Li Zhong , Dantong Lv, Weizhen Zhan, Muhammad Amjad, Xin Meng and Haiyan Zhang*

*E-mail: zhanghy@cmu.edu.cn

Received 25 June 2026; Revised 20 October 2026; Accepted 9 November 2026; Published 20 November 2026

https://doi.org/10.55092/ijee20260017

Graphical Abstract



Highlights:

- PFOA impaired angiogenesis in HUVECs and caused aortic intimal damage in mice.
- PFOA suppressed PKA/GSK-3β/β-catenin/Snail signaling in endothelial cells.
- Loss of nuclear β-catenin and Snail drove the anti-angiogenic effect.

Copyright© 2026 by the authors. Published by ELSP. This work is licensed under Creative Commons Attribution 4.0 International License, which permits unrestricted use, distribution, and reproduction in any medium provided the original work is properly cited.

PFOA impairs angiogenesis via PKA/GSK-3β/β-catenin/Snail signaling, revealing a novel mechanism for cardiotoxicity

He Xiao[1,†], Yixuan Liu[2,†], Lujiao Yu[1,†], Li Zhong[3], Dantong Lv[4], Weizhen Zhan[5], Muhammad Amjad[6], Xin Meng[7] and Haiyan Zhang[1,*]

[1] Department of Geriatrics, The First Hospital of China Medical University, Shenyang, China

[2] Department of Gerontology and Geriatrics, Shengjing Hospital of China Medical University, Shenyang, China

[3] Department of Public Health, China Medical University, Shenyang, China

[4] Bolyn Biomedical Research Institute, Shenyang, China

[5] Hospital of Stomatology, China Medical University, Shenyang, China

[6] Joint International Research Laboratory of Environment and Health, Ministry of Education, Guangdong Provincial Engineering Technology Research Center of Environmental Pollution and Health Risk Assessment, Department of Occupational and Environmental Health, School of Public Health, Sun Yat-sen University, Guangzhou, China

[7] Department of Biochemistry and Molecular Biology, School of Life Sciences, China Medical University, Shenyang, China

† These authors contributed equally to this work.

*E-mail: zhanghy@cmu.edu.cn.

International Journal of Environmental Epidemiology

Abstract: **Background:** Perfluorooctanoic acid (PFOA) is a widespread environmental contaminant associated with cardiovascular disease risk. However, the direct impact of PFOA on endothelial dysfunction and angiogenesis, critical processes in cardiovascular pathogenesis, remains poorly understood. **Methods:** Using a mouse model and human umbilical vein endothelial cells (HUVECs), we assessed aortic intimal damage, endothelial functions (proliferation, migration, tube formation), and performed RNA-sequencing to uncover the underlying mechanisms. **Results:** *In vivo*, PFOA exposure caused aortic intimal damage and significantly elevated blood pressure and aortic inflammatory/oxidative stress markers in mice. *In vitro*, PFOA inhibited HUVEC angiogenesis in a concentration-dependent manner (24 h, IC_{50} = 463 μM), significantly reducing cell viability, migration, and tube formation at a subcytotoxic concentration of 40 μM. Mechanistically, PFOA suppressed PKA and GSK-3β phosphorylation, prevented β-catenin nuclear translocation, and downregulated Snail expression; restoration of these signaling nodes rescued the angiogenic defects. **Conclusion:** Our findings demonstrate that PFOA impairs angiogenesis by suppressing the PKA/GSK-3β/β-catenin/Snail signaling axis, revealing a novel mechanism for PFOA-induced cardiotoxicity and providing potential targets for intervention.

Keywords: perfluorooctanoic acid (PFOA); cardiotoxicity; endothelial dysfunction; angiogenesis; PKA/GSK-3β signaling; β-catenin

1. Introduction

Perfluorooctanoic acid (PFOA) is a member of the Per- and polyfluoroalkyl substances (PFASs), a class of synthetic compounds known for their extreme resistance to degradation [1,2]. PFOA is characterized by its exceptional chemical stability and its hydrophobic and oleophobic properties, which come from the unique carbon-fluorine bonds in its molecular structure [2,3]. Thus, it has been commonly used in various fields, including aviation technology, transportation, surfactants, waterproof coatings, and kitchen utensils [1,4]. Due to its persistence and extensive application, PFOA accumulates in the environment through the food chain and has been detected in air, groundwater, river, soil and fishes, even spreading to remote areas, such as the Arctic or Antarctic [2,5,6].

Human exposure to PFOA is quite widespread, mainly through dietary sources, drinking water, and respiration [7]. PFOA is quickly absorbed by organisms but is difficult to eliminate, with an estimated half-life in humans ranging from 1.48 to 5.1 years [8]. This leads to lasting persistent health effects, including endocrine disruption, inflammation, immune response, and cytotoxicity [9–11].

Given these well-documented health hazards, PFOA raises substantial environmental and public health concerns. Many studies have shown that PFOA contributes to significant environmental pollution and causes developmental toxicity in various species, including reproductive toxicity, hepatotoxicity, cardiotoxicity, neurotoxicity, and immunotoxicity [2,12,13].

Cardiovascular diseases (CVDs), as the leading threat to human health worldwide, have been linked to exposure to environmental pollutants, including PFOA [14,15]. It has been reported that exposure to PFOA can cause oxidative stress, disruptions in lipid metabolism, developmental toxicity, and immune toxicity in organisms [16]. A strong association exists between PFOA exposure and an increased risk of hypertension, hypercholesterolemia, and hyperuricemia [14]. Recently, several studies have highlighted the cardiovascular toxicity of PFASs. Jing Yu *et al.* showed that heart rate and motor behavior significantly decreased when zebrafish embryos were exposed to PFOA and identified target cell populations through single-cell RNA sequencing analysis [17]. High-throughput proteomics research further revealed that PFOA exposure concurrently impairs heart morphogenesis and function [18]. In avian models, PFOA exposure induced severe cardiotoxicity during development, causing right ventricular remodeling and dysregulation of key cardiac development genes [19,20]. These findings suggest that PFOA can induce developmental cardiotoxicity in vertebrates, although the underlying toxic mechanisms remain unclear. Nevertheless, existing animal studies mainly focused on cardiac developmental abnormalities, and it remains undetermined whether vascular endothelial dysfunction serves as an early intermediate event linking PFOA exposure to subsequent cardiovascular and cardiac injury.

Endothelial angiogenesis, defined as the growth of new blood vessels from pre-existing vasculature, is a core determinant of vascular function and a critical early event in the pathogenesis of cardiovascular diseases [21]. It involves the coordination of endothelial cell proliferation, migration, and tube formation. This intricate physiological process is managed by multiple signaling pathways. Vascular endothelial growth factor (VEGF) is one of the key regulators in angiogenesis [22]. The Notch signaling pathway controls the specialization, proliferation, migration, adhesion, and arteriovenous differentiation of endothelial cells [23]. Additionally, the platelet-derived growth factor (PDGF) family influences various aspects of angiogenesis [24]. However, whether PFOA disrupts angiogenesis and thereby triggers vascular dysfunction as an upstream contributor to its cardiotoxicity remains poorly characterized, requiring further mechanistic investigation.

Of note, the PKA/GSK-3β/β-catenin/Snail signaling cascade is a well-characterized axis that tightly governs endothelial homeostasis and angiogenic activity. Activation of PKA promotes GSK-3β phosphorylation and inactivation, which stabilizes β-catenin and facilitates its nuclear translocation to modulate the transcription of Snail and other angiogenic-related genes. Dysregulation of this signaling cascade contributes to endothelial dysfunction, impaired angiogenesis, and aortic remodeling, which are closely implicated in the initiation and progression of cardiovascular lesions. Despite its established role in vascular biology, whether PFOA disrupts endothelial angiogenesis through modulation of the PKA/GSK-3β/β-catenin/Snail axis remains unexplored.

Given the above unresolved questions, the present study aimed to clarify the causal link between PFOA exposure, endothelial angiogenic dysfunction, and subsequent cardiotoxicity. We hypothesized that PFOA impairs vascular endothelial angiogenesis via the regulation of key intracellular signaling cascades, thereby driving aortic intimal damage and vascular dysfunction, which serves as a critical mechanistic basis for PFOA-induced cardiovascular toxicity. To verify this hypothesis, we established an *in vivo* PFOA-exposed mouse model to evaluate aortic structural and functional injury, combined with *in vitro* HUVEC experiments to explore the underlying molecular mechanism. This study provides novel mechanistic insights into PFOA-associated vascular cardiotoxicity and offers potential therapeutic targets for the prevention of environmental pollutant-induced vascular injury.

2. Methods and materials

(1) Animals and treatment

C57BL/6 male mice at 8 weeks were purchased from OBiO Technology Company (Shanghai, China). The mice were randomly divided into two groups: the control group (control) and the PFOA group (PFOA). Each group included 8 mice, and all animals had free access to food and water. Over 9 weeks, mice in the PFOA group were exposed to a PFOA mixture in drinking water, while the control group received only water. PFOA (Product No. 171468, Sigma-Aldrich, USA) was dissolved in water at a concentration of 5 mg/L with water bottles replaced weekly. This dosing aimed to reach serum PFOA levels similar to those found in people with high occupational exposure, such as workers at PFAS manufacturing plants, where serum PFOA ranges from 1.3 to 12.9 μg/mL [25,26]. The present study focused on exploring the toxic mechanism of high-risk occupational PFOA exposure-induced vascular endothelial injury and cardiotoxicity. Therefore, a single occupationally relevant concentration was adopted for *in vivo* modeling to eliminate the interference of dose gradient variables and specifically clarify the core toxic phenotype and molecular mechanism. General environmental low-dose PFOA exposure was not included in this study, as subtle vascular changes induced by low-level environmental exposure are difficult

to stably observe within a short-term animal experiment and are more suitable for long-term population epidemiological investigation and chronic low-dose animal studies in the future. After 9 weeks, mice were euthanized under anesthesia by cervical dislocation, and tissues were collected for analysis. Only male mice were used in this study to avoid confounding by sex-specific hormonal cycles. The results may not be generalizable to female mice, and future studies including both sexes are needed to assess potential sex differences in PFOA-induced cardiotoxicity.

(2) Blood pressure measurement

Systolic and diastolic blood pressure (SBP and DBP) were measured in conscious, restrained mice from both the control and PFOA groups (n = 8 per group) using the non-invasive tail-cuff system (CODA 8, Kent Scientific, Torrington, CT, USA). To minimize stress-induced variations, all mice were acclimated to the restraining device and measurement procedure for 30 minutes daily over 3 consecutive days prior to formal data collection. Blood pressure measurements were performed weekly throughout the 9-week exposure period. For each recording session, at least five stable consecutive readings were obtained and averaged for every mouse.

(3) Detection of tissue biochemical indices

Aortic tissue (100 mg) was weighed and homogenized with 1 mL of lysis buffer. The homogenate was centrifuged at 8000 × g for 10 minutes, and the supernatant was collected. Superoxide dismutase (SOD), malondialdehyde (MDA) and glutathione peroxidase (GSH-Px) were detected according to the kit instructions provided by Solarbio Life Sciences (n = 8).

(4) Histological analysis

Aortic arch tissue sections were collected from each group. After dewaxing with xylene and soaking in graded alcohol solutions concentrations, the tissues were stained with hematoxylin–eosin. The slides were dehydrated, cleared with xylene, covered with a cover slip, sealed with neutral adhesive, and examined under a Leica DM500 optical microscope.

(5) Cell culture and treatment

HUVECs were obtained from the Cell Bank of the Chinese Academy of Sciences (Shanghai, China) and cultured in growth medium, consisting of RPMI 1640 medium (Biological Industries, Israel), 10% fetal bovine serum (Product No. A5256701, Thermo Fisher Scientific) and 1% penicillin-streptomycin, in a 5% CO_2 atmosphere, at 37 °C. The cells were then treated with PFOA at concentrations of 0, 5, 10, 50, 100, 200, and 400 μM for 24, 48, or 72 hours. This concentration range was designed to span a wide dose–response window around the anticipated IC_{50}. In preliminary experiments, 400 μM produced approximately 50% inhibition of HUVEC viability at 24 h, close to the half-maximal inhibitory range; this concentration was therefore set as the highest dose so that the full dose–response curve, including the near-IC_{50} region, could be fitted for reliable IC_{50} estimation. The 24-h IC_{50} value of PFOA in HUVECs was calculated as 463 μM via CCK-8 detection and nonlinear regression analysis. Although 40 μM was not included in the main dose–response series (0–400 μM) designed for IC_{50} fitting, its subcytotoxic nature was verified in three independent experiments, in which 24-h cell viability remained at 99.60% ± 0.50% of the control. This concentration, well below the 24-h IC_{50} (463 μM), was therefore selected for the subsequent mechanistic experiments to exclude confounding by general cytotoxicity. In some experiments, cells were pre-treated with 0.2, 0.4, 0.8 or 1 mM 8-Bromo-cAMP (Product No. HY-12306A, MCE, USA) or 2, 5, 10, 15 mM LiCl (Product No. 213233, Sigma-Aldrich, USA) for 24 hours before PFOA exposure.

(6) Plasmids, lentiviral infection, and transfection

Human β-*catenin* or *Snail* cDNA was amplified by PCR and cloned into the pSin-EF2 lentiviral vector. We then generated stable cell lines overexpressing either β-*catenin*, *Snail*, or a nuclear-localized variant of β-*catenin*, along with their corresponding control lines. All stable cell lines were selected and maintained using 0.5 mg/mL puromycin.

(7) CCK-8 assays

Cells were plated in 96-well plates at a density of 3000 cells per well. PFOA (0, 5, 10, 50, 100, 200, and 400 μM) was added to the cultures 24 hours after seeding. After an additional 24, 48, and 72 hours of incubation, 10 μL of CCK-8 solution (Cat No. K2268, APExBIO, USA) was added to each well, and the plates were incubated in the dark at 37 °C for 3 hours. Absorbance was measured at 450 nm using a microplate reader. Cell viability was expressed as the percentage of the untreated control (0 μM, set as 100%) for each time point. The 24-h IC_{50} was calculated by nonlinear regression using the "[Inhibitor] *vs.* normalized response—variable slope" (four-parameter logistic) model in GraphPad Prism 9.0.

(8) Quantitative real-time PCR

Total RNA was extracted from mouse aorta tissue and HUVECs using the Qiagen RNeasy Mini Kit, coupled with on-column DNase treatment (Applied Biosystems, USA). Reverse transcription was carried out using a cDNA Reverse Transcription Kit (Product No. 4374966, Thermo Fisher Scientific). Quantitative real-time PCR was performed with the Power SYBR Green PCR Master Mix (Applied Biosystems, USA) and a LightCycler® 480 Real-time PCR system (Roche, Basel, Switzerland). Sequences of primers used for qPCR amplification of target and reference genes are summarized in Table 1. The expression of target genes was normalized to reference genes (*GAPDH* and *18S*), and the relative fold change was calculated using the 2−ΔΔCT method.

Table 1. Primer sequences used for qPCR analysis.

Gene	Forward Primer (5'-3')	Reverse Primer (5'-3')
IL-6	GCC ACT CAC CTC TTC AGA ACG AAT T	GGC AAG TCT CCT CAT TGA ATC CAG AT
IL-1β	TGA TGG CTT ATT ACA GTG GCA	GGT CGG AGA TTC GTA GCT GG
TNF-α	CTC TTC TGC CTG CTG CAC TTT G	ATG GGC TAC AGG CTT GTC ACT C
VEGFA	CTT CGC TTA CTC TCA CCT GCT TCT G	GCT GCT TCT TCC AAC AAT GTG TCT CT
VEGFR2	CTG GCT ACT TCT TGT CAT CAT CCT ACG	TGG CAT CAT AAG GCA GTC GTT CAC
MMP-2	CGA CCA CAG CCA ACT ACG ATG ATG	AGA CGG AAG TTC TTG GTG TAG GTG TA
MMP-9	GAG TTG AAC CAG GTG GAC CAA GTG	CTC CTC CCT TTC CTC CAG AAC AGA A
VCAM-1	CCT GAA TCC CAG CGA ATT CC	TCC TCT TTG GGC TTG TTC TC
ICAM-1	TGG CAG CAC TGA ACG TGA G	GGC TCG CAG GTC AAA GTT G
N-cadherin	TGC GGT ACA GTG TAA CTG GG	GAA ACC GGG CTA TCT GCT CG
Snail	TCG GAA GCC TAA CTA CAG CGA	AGA TGA GCA TTG GCA GCG AG
18S	GCA GAA TCC ACG CCA GTA CAA GAT	TCT TCT TCA GTC GCT CCA GGT CTT
GAPDH	TCG CTC TCT GCT CCT CCT GTT C	CCG TTG ACT CCG ACC TTC ACC T

(9) Western blotting

Cells and tissues were lysed in cold radioimmunoprecipitation assay (RIPA) buffer containing protease inhibitors. Approximately 40 μg of total protein was denatured and separated by 10% SDS-PAGE, then transferred onto a nitrocellulose membrane. The membranes were blocked with 5% skim milk for 1 hour at room temperature, and subsequently incubated overnight at 4 °C with the following primary antibodies: PKA, p-PKA, GSK-3β, p-GSK-3β (Ser9), PDK1, p-PDK1 (Ser241), YAP, p-YAP (Ser127), VE-Cadherin, N-Cadherin, vimentin, and Snail (Cat. No. #4782, #4781, #9315, #9336, #3062, #3061, #4912, #4911, #2158, #4061, #3932, #3879, Cell Signaling Technology, USA). GAPDH and β-actin (Cat No. #2118, #4970, Cell Signaling Technology, USA) were used as loading controls. The membranes were incubated with horseradish peroxidase-conjugated secondary antibodies for 1 hour at room temperature. Protein signals were visualized using an ECL kit (Beyotime Biotechnology, Shanghai, China) and detected with a Chemiluminescence Imaging Analysis System (Tanon, Shanghai, China).

(10) Scratch wound healing assays

Cells subjected to the specified treatments were seeded in 6-well plates and incubated overnight. Once the cells reached approximately 100% confluence, a wound was created by gently scraping the monolayer with a 10 μL pipette tip. The cells were then washed with PBS to remove any debris. Cell migration into the wound area was monitored at 24 and 48 hours after scraping by taking images with an inverted microscope. Wound healing percentages at each time point were calculated using ImageJ software.

(11) Tube formation assays

Growth factor-reduced Matrigel (Corning, USA) was gently added to the selected wells of a 96-well plate. HUVECs (20,000 cells/well) were seeded onto the surface of the Matrigel matrix and treated with the indicated chemicals. After incubation at 37 °C for 1, 2, and 3 hours, images were captured and analyzed using ImageJ software to assess tube formation.

(12) Immunofluorescence

Cells were fixed with 4% paraformaldehyde, permeabilized in 0.2% Triton X-100, and blocked with 15% bovine serum albumin (BSA) for 30 minutes. The coverslips were incubated overnight at 4 °C in the dark with DAPI (Cat No. PR30021, Proteintech, USA) or primary antibodies against β-catenin (Cat No. #9562, Cell Signaling Technology, USA). Immunofluorescence images were captured using a fluorescence microscope (BX63, Olympus, Japan).

(13) HUVECs RNA extraction, library preparation and sequencing

RNA was extracted from HUVECs using the RNA Library Kit (Vazyme, China). The extracted RNA was eluted with RNase free water and stored at −80 °C. A total of 500 ng of RNA was used as input for library preparation, following the manufacturer's protocol.

(14) Bioinformatic data analysis

RNA-Seq data analysis was performed using CLC Genomics Workbench v10.1.1 (CLC bio, Denmark) in accordance with the developer's protocol. In short, raw single-end reads in FASTQ format underwent quality assessment with the "QC for Sequencing Reads" module. The cleaned reads were then aligned to the human reference genome (GRCh38/hg38) using the default settings of the "RNA-Seq Analysis" pipeline, with gene

annotations from Ensembl release 109. To identify differentially expressed genes (DEGs) between the control and PFOA-treated HUVECs groups, the "Differential Expressions in Two Groups" function was utilized, employing a negative binomial generalized linear model. Genes with a false discovery rate (FDR)-adjusted P-value ≤ 0.05 and an absolute $\log_2$ fold change ≥ 1.2 were classified as DEGs. Only genes exhibiting consistent expression changes across all three biological replicates were considered for subsequent analysis. Pathway enrichment analysis was performed using Ingenuity Pathway Analysis (IPA®, QIAGEN, USA). Functional annotation and gene set enrichment were further conducted via the Database for Annotation, Visualization, and Integrated Discovery (DAVID) [27], using the human genome as the background reference. A significance threshold of $P < 0.05$ and a minimum gene count of 2 were applied.

(15) Statistics

Data are presented as mean ± SEM. Normality was assessed using the Shapiro–Wilk test. Differences between two groups were analyzed by two-tailed unpaired Student's t-test, or by the Mann–Whitney U test when data were not normally distributed. For comparisons among three or more groups, one-way analysis of variance (ANOVA) followed by Tukey's post hoc test was used; when multiple treatment groups were compared against a single control, Dunnett's post hoc test was applied. For the CCK-8 assay involving multiple concentrations and time points, two-way ANOVA followed by Dunnett's post hoc test was used. A P value of less than 0.05 was considered statistically significant. All statistical analyses were performed using GraphPad Prism 9.0 (GraphPad Software, San Diego, CA, USA).

3. Results

3.1. PFOA exposure induces aortic intimal damage

To investigate the toxic effects of PFOA on vascular function, we first assessed physiological and structural changes in the mouse aorta after 9 weeks of exposure. Histological examination revealed an irregular and less smooth endothelial lining, disrupted arrangement of endothelial cells, and thickening of the medial layer in PFOA-treated mice. Additionally, the smooth muscle cells in the PFOA exposure group displayed increased thickness, disorganized arrangement, and variations in nuclear size (Figure 1A). Furthermore, PFOA-exposed mice exhibited significant increases in both systolic and diastolic blood pressure (SBP and DBP) compared to the control group (Figure 1B). Moreover, PFOA exposure significantly upregulated inflammatory factors and oxidative stress markers in the mouse aorta compared to the control group (Figure 1C,E). Decreased mRNA expression of angiogenic factors (VEGFA, VEGFR2) was observed in the PFOA-exposed mouse aorta (Figure 1D). These findings collectively suggest that PFOA exposure induces hypertension and causes significant damage to the aortic structure and function.

3.2. PFOA inhibits the angiogenesis of HUVECs

To assess the toxic effects of PFOA on HUVECs, we first determined its half-maximal inhibitory concentration (IC_{50}) to be 463 μM (Figure 2A). Cells were then incubated with PFOA at concentrations ranging from 0 to 400 μM for 24, 48, and 72 hours, and viability was measured using the CCK-8 assay. As shown in Figure 2B, PFOA inhibited cell proliferation in a dose-dependent manner, with 400 μM significantly suppressing growth within 24 hours. Because 40 μM is well below the 24-h IC_{50} (463 μM) and maintained cell viability at 99.60% ± 0.50% of the control in three independent experiments, this subcytotoxic concentration was selected for the subsequent mechanistic experiments. We next examined the impact of PFOA on tube formation and migration. The tube-formation assay revealed that PFOA treatment resulted in fewer vascular-like structures and branch points (Figure 2C,D). Similarly, the wound healing assay showed that PFOA exposure significantly impeded cell migration (Figure 2E,F). These findings collectively indicate that PFOA inhibits angiogenesis in HUVECs *in vitro*.

3.3. Verification of RNA-seq-based mechanism of HUVECs on PKA signaling pathway

To further investigate the mechanisms by which PFOA inhibits angiogenesis, RNA-seq was performed on purified HUVECs. Given that mouse aortic tissue contains multiple cell subtypes, bulk RNA-seq of whole aortas cannot distinguish endothelial-specific transcriptional changes. Homogeneous HUVECs were therefore used for transcriptomic screening of endothelial-autonomous mechanisms, followed by validation of key targets in mouse aortic tissue via qPCR and Western blot. We extracted mRNA from control and PFOA-treated HUVECs to construct a transcriptome library, which involved RNA isolation, fragmentation, dsDNA synthesis, ligation, and high-throughput sequencing. As shown in the volcano plot, the sequencing data analysis identified 463 differentially expressed genes (DEGs) in the PFOA treated groups compared to the control group, including 273 upregulated genes and 190 downregulated genes (Figure 3A,B). Gene set enrichment analysis (GSEA) was implemented to identify enriched pathways, revealing a significant association between PFOA exposure and the PKA signaling pathway ($P = 0.005$, $NES = -1.72$; Figure 3C). Consequently, we hypothesized that the PKA signaling pathway plays a role in PFOA's inhibitory effects on angiogenesis.

To validate the hypothesis, the protein expression of total PKA (PKA) and phosphorylated PKA (p-PKA) was examined by WB analysis in PFOA-treated HUVECs. As shown in Figure 3D,E, there was no significant change in the expression of PKA, but the levels of p-PKA were significantly reduced in the PFOA-treated group compared to the control. Overall, these results indicate that PFOA may inhibit the phosphorylation and activity of PKA in HUVECs, and implicate the PKA signaling pathway in the regulation of angiogenesis following PFOA exposure.

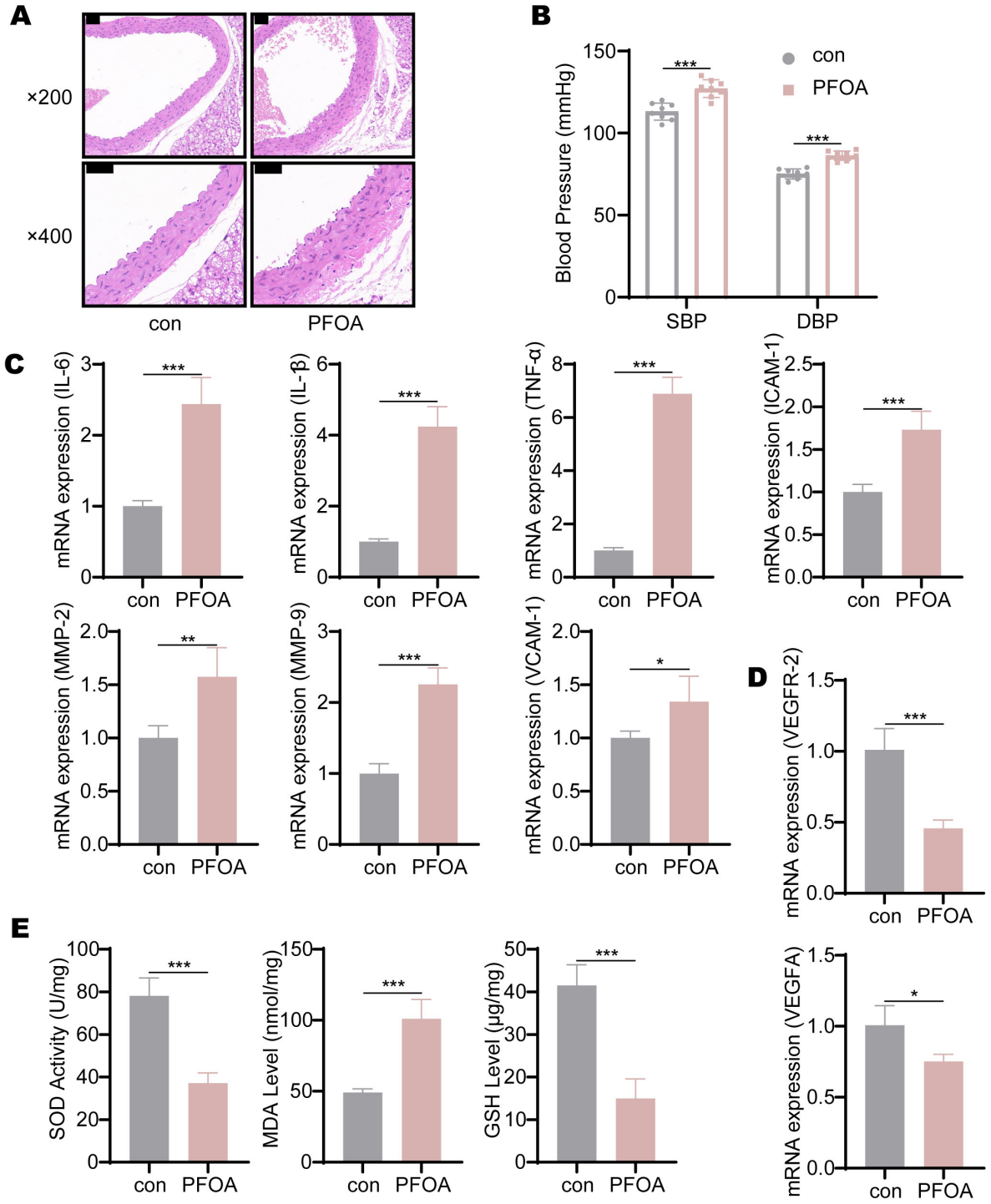


Figure 1. Effects of PFOA exposure on aortic intimal damage of mice. **(A)** HE staining of representative aortic arch sections. The scale bar represents 100 μm; **(B)** Measurements of systolic and diastolic blood pressure (SBP and DBP) after 9 weeks of exposure (n = 8); **(C, D)** Aorta gene expression of IL-6, IL-1β, TNF-α, VEGFA, VEGFR2, MMP-2, MMP-9, VCAM-1, ICAM-1 in each group. n = 8 mice per group; **(E)** Detection of superoxide dismutase (SOD) activity, MDA levels and glutathione peroxidase (GSH-Px) activity in aortic tissue. Data are represented as the mean ± SEM. *P < 0.05, **P < 0.01, ***P < 0.001.

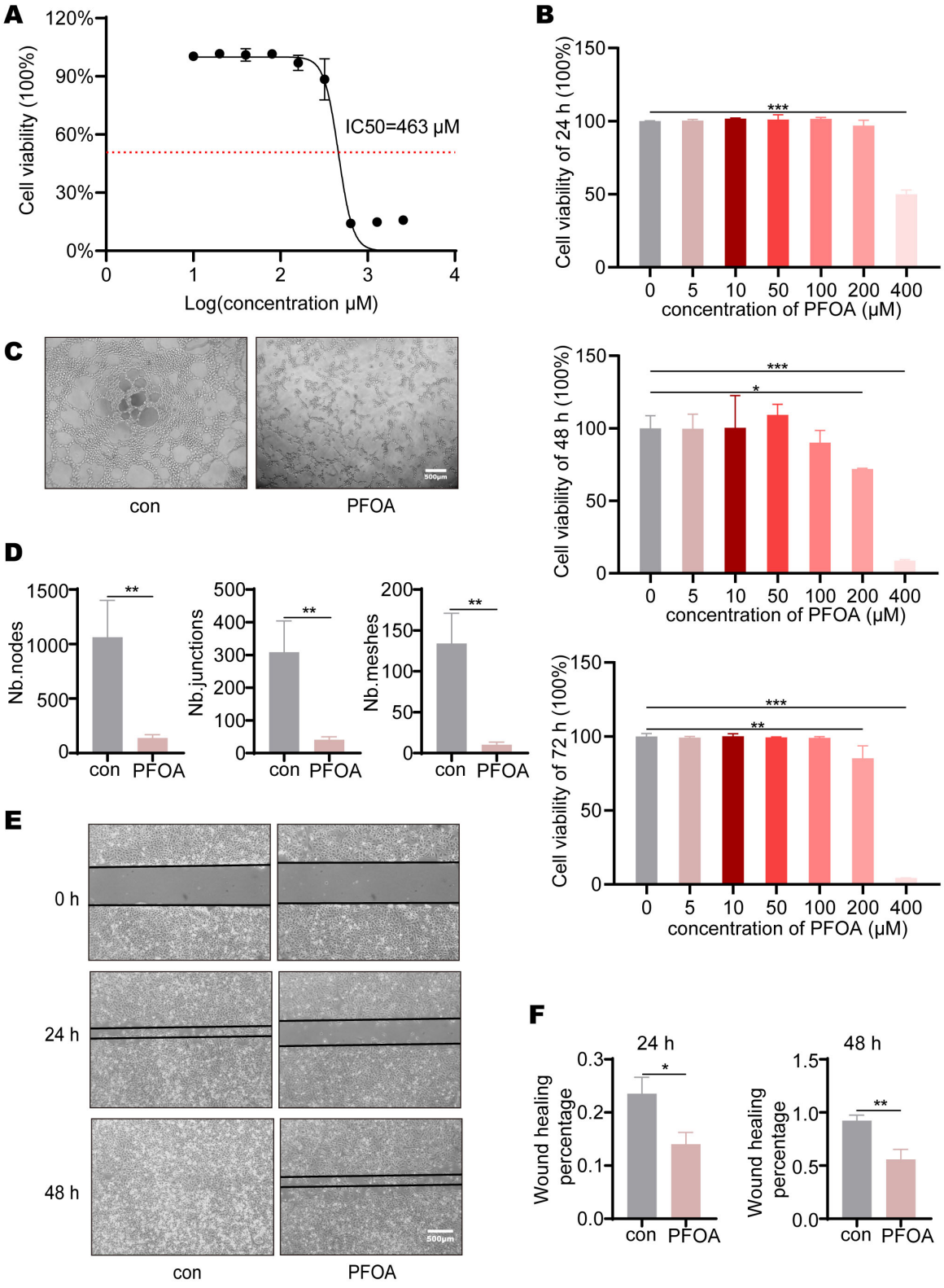


Figure 2. Effects of PFOA on angiogenesis of HUVECs. **(A)** The cytotoxic effect of PFOA on HUVECs was determined by CCK-8 assay after 24 h of exposure. The 24-h IC_{50} of PFOA was 463 μM, calculated by nonlinear regression using a four-parameter logistic model, with viability normalized to the untreated control (100%); **(B)** HUVECs were exposed with the indicated concentrations of PFOA for 24 h, 48 h and 72 h, and then cell viability was measured by CCK-8 assay; **(C, D)** In the tube formation assay, HUVECs were treated with PFOA (40 μM) for 24 hours and photographed after 3 hours (n = 3). Bars indicate 500 μm; **(E, F)** In the scratch assay, HUVECs were treated with PFOA (40 μM) and photographed at 0, 24, and 48 hours (n = 3). Bars indicate 500 μm. Data are represented as the mean ± SEM. *P < 0.05, **P < 0.01, ***P < 0.001.

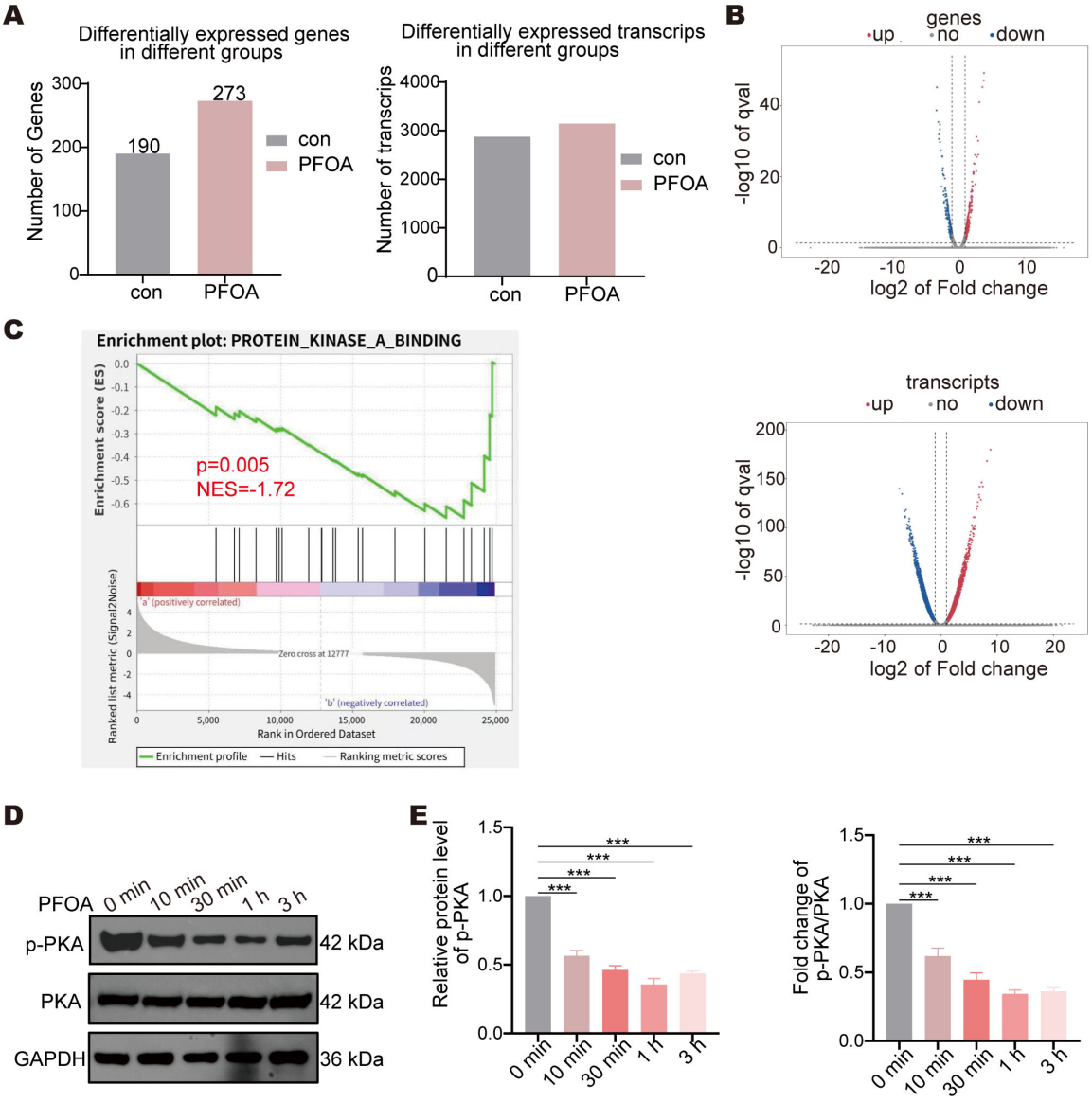


Figure 3. Transcriptome effects of PFOA in HUVECs. **(A)** The differentially expressed genes and transcripts in PFOA-treated HUVECs and control group (FDR-adjusted P ≤ 0.05 and $|\log_2 FC| \geq 1.2$); **(B)** Volcano plot analysis of PFOA-treated group and control group in HUVECs; **(C)** Gene set enrichment analysis (GSEA) showing enrichment of the PKA signaling pathway in PFOA-treated HUVECs compared with the control group (P = 0.005, NES = −1.72); **(D, E)** Representative western blots showing p-PKA, PKA. Quantitative analysis of p-PKA/PKA protein expression levels in HUVECs after PFOA at different time. Data are represented as the mean ± SEM. *P < 0.05, **P < 0.01, ***P < 0.001.

3.4. PFOA inhibits the angiogenesis through attenuating the phosphorylation of PKA in HUVECs

To further validate the involvement of the PKA signaling pathway in PFOA-induced angiogenesis impairment, we stimulated HUVECs with 8-Bromo-cAMP (8-BA), a PKA activator. As expected, 8-BA treatment increased the level of phosphorylated PKA (p-PKA) in a concentration-dependent manner (Figure 4A,B). A maximal increase in p-PKA was observed at 0.8–1 mM (Figure 4A,B); therefore, 1 mM 8-BA was selected for the subsequent rescue experiments. This concentration is within the range commonly used for 8-Bromo-cAMP in endothelial cell studies [28]. We then investigated whether activating PKA could rescue the angiogenic defects caused by PFOA. Wound healing and tube formation assays demonstrated that co-treatment with 8-BA significantly restored the migration capacity (Figure 4E,F) and increased the number of capillary-like structures (Figure 4C,D) in PFOA-exposed HUVECs, compared to the PFOA-only group. Collectively, these results suggest that PFOA impairs angiogenesis in HUVECs by suppressing PKA phosphorylation.

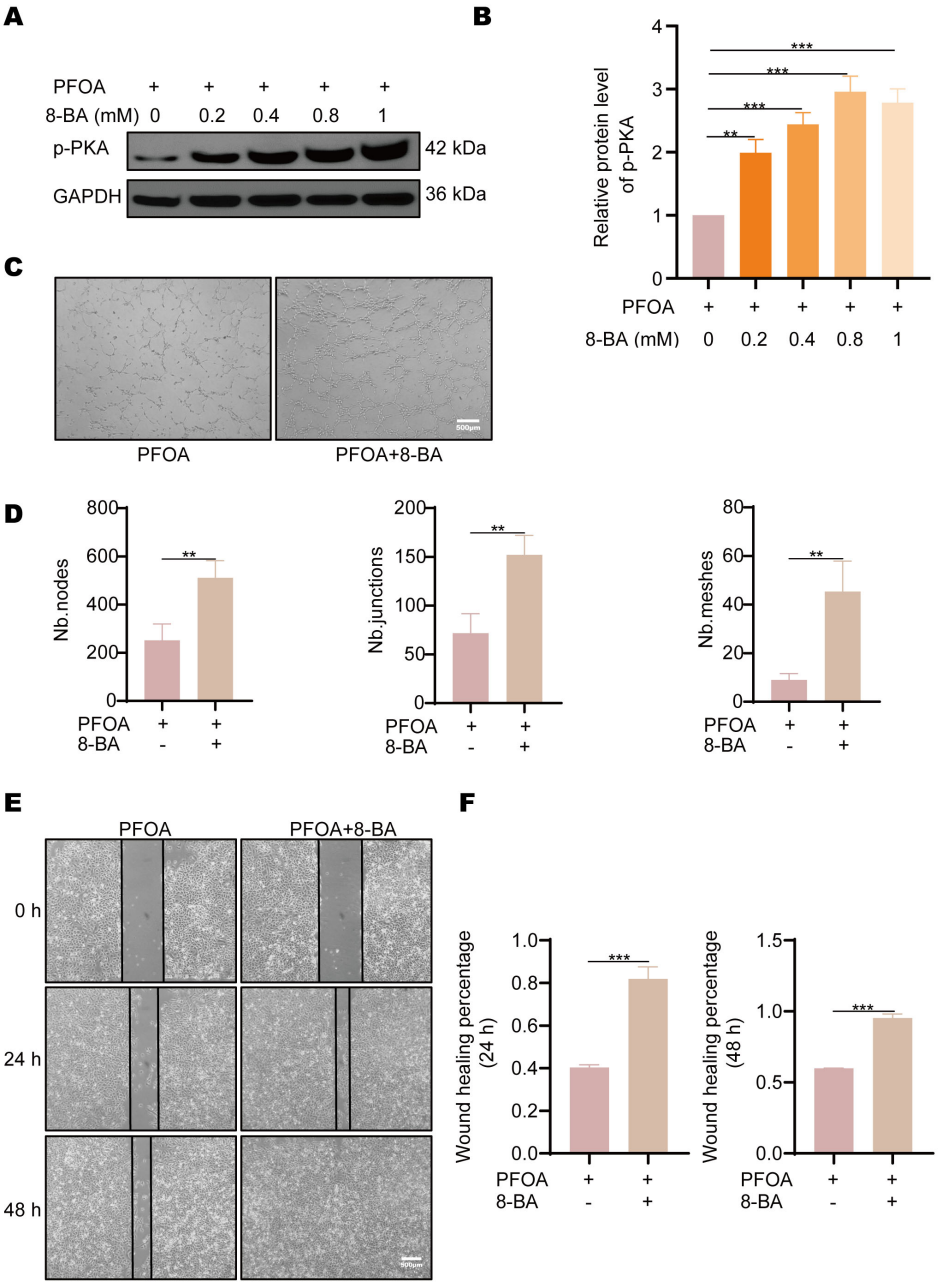


Figure 4. Effects of the activator of PKA on angiogenesis in HUVECs exposed with PFOA. **(A, B)** HUVECs were exposed with the indicated concentrations of 8-BA and PFOA (40 μM) for 24 h and then the expression of p-PKA and GAPDH were detected by western blot; **(C, D)** In the tube formation assay, HUVECs were treated with PFOA and 8-BA, or not, for 24 hours and photographed after 3 hours (n = 3). Bars indicate 500 μm; **(E, F)** In the scratch assay, HUVECs were treated with PFOA and 8-BA (1 mM), or not, and photographed at 0, 24, and 48 hours (n = 3). Bars indicate 500 μm. Data are represented as the mean ± SEM. *P < 0.05, **P < 0.01, ***P < 0.001.

3.5. PFOA inhibits the angiogenesis via suppressing the phosphorylation of GSK-3β in HUVECs

Our previous results established that the suppression of PKA signaling is crucial for the anti-angiogenic effect of PFOA in HUVECs. Since several downstream effectors of PKA, including GSK-3β, YAP, and PDK1, are involved in angiogenesis, we sought to determine which of these are implicated in PFOA's action. Western blot analysis revealed that PFOA significantly inhibited the phosphorylation of GSK-3β at Ser9 (p-GSK-3β), thereby activating its kinase activity, while the phosphorylation states of YAP and PDK1 were unaffected (Figure 5A,B). To confirm that GSK-3β is a downstream target of PKA in this context, we treated HUVECs with the PKA activator 8-BA. This treatment significantly restored the levels of p-GSK-3β (Ser9) that were reduced by PFOA (Figure 5C,D). Collectively, these findings demonstrate that PFOA attenuates the inhibitory phosphorylation of GSK-3β at Ser9, thereby increasing its kinase activity, a mechanism mediated through the inhibition of PKA phosphorylation.

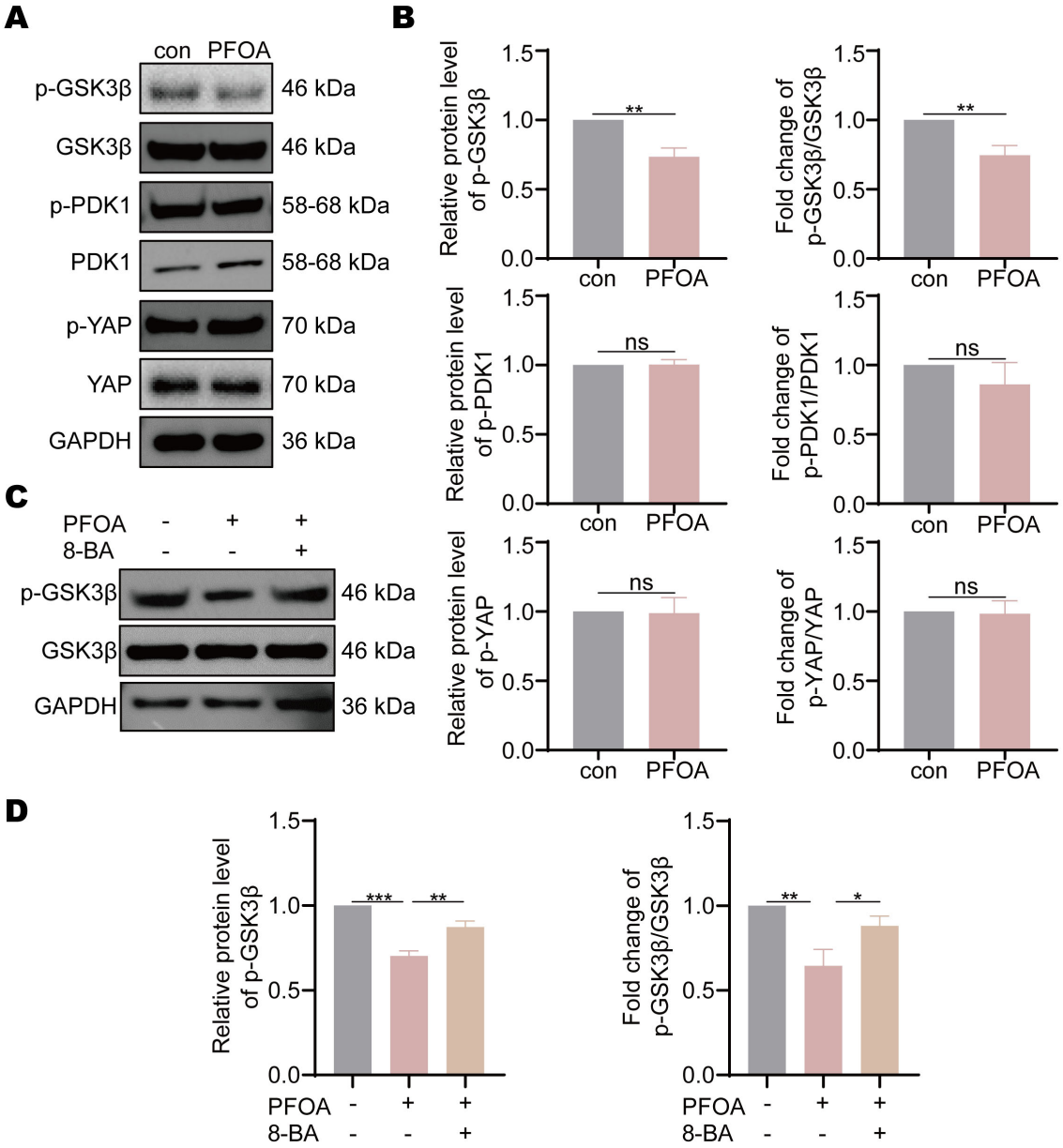


Figure 5. Protein expression level of the PKA downstream signaling pathway in HUVECs treated with PFOA. **(A, B)** HUVECs were treated with the PFOA (40 μM) and control for 24 h, then the expression of p-GSK-3β, GSK-3β, p-PDK1, PDK1, p-YAP, YAP, and GAPDH were detected by western blot; **(C, D)** HUVECs were treated with the PFOA, 8-BA (1 mM) and control for 24 h, then the expression of p-GSK-3β, GSK-3β and GAPDH were detected by western blot. Data are represented as the mean ± SEM. *P < 0.05, **P < 0.01, ***P < 0.001.

To confirm the functional role of GSK-3β hyperactivation, we treated the cells with LiCl, a known GSK-3β inhibitor. LiCl promotes the inhibitory phosphorylation of GSK-3β at Ser9, thereby effectively suppressing its kinase activity. As shown in Figure 6A,B, LiCl treatment rescued the level of p-GSK-3β (Ser9) that was reduced by PFOA. Consequently, this pharmacological inhibition of GSK-3β restored tube formation and cell migration (Figure 6C–F).

Notably, GSK-3β activity is tightly controlled by Ser9 inhibitory phosphorylation: phosphorylation at Ser9 completely inactivates GSK-3β, whereas dephosphorylation at this site maintains its constitutive kinase activity under basal conditions. In the canonical Wnt signaling cascade, active GSK-3β forms a cytoplasmic destruction complex with APC and Axin, which continuously phosphorylates cytosolic β-catenin and targets it for ubiquitination and proteasomal degradation. Therefore, the PFOA-mediated reduction in GSK-3β (Ser9) phosphorylation sustains GSK-3β activation, promotes persistent β-catenin degradation in the cytoplasm, and ultimately blocks β-catenin nuclear translocation. Mechanistically, PKA acts as an upstream positive regulator of this axis; suppressed PKA signaling directly reduces GSK-3β Ser9 phosphorylation and releases GSK-3β from its inactive state, establishing a definitive PKA/GSK-3β/β-catenin regulatory cascade in PFOA-induced endothelial dysfunction.

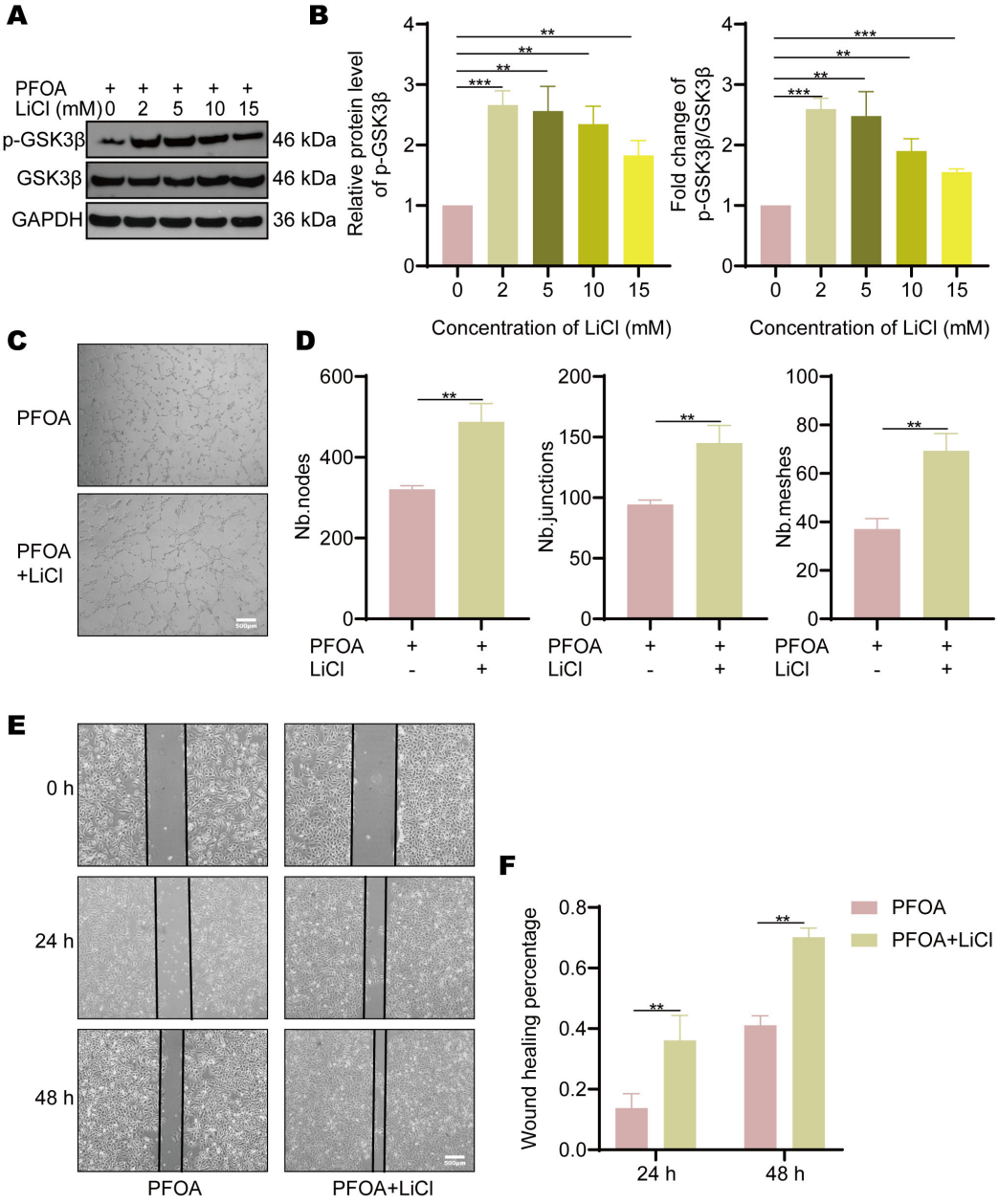


Figure 6. Effects of the activator of GSK-3β on angiogenesis in HUVECs treated with PFOA. **(A, B)** HUVECs were exposed with the indicated concentrations of LiCl and PFOA (40 μM) for 24 h and then the expression of GSK-3β, p-GSK-3β and GAPDH were detected by western blot; **(C, D)** In the tube formation assay, HUVECs were treated with PFOA (40 μM) and LiCl, or not, for 24 hours and photographed after 3 hours (n = 3). Bars indicate 500 μm; **(E, F)** In the scratch assay, HUVECs were treated with PFOA (40 μM) and LiCl (2 mM), or not, and photographed at 0, 24, and 48 hours (n = 3). Bars indicate 500 μm. Data are represented as the mean ± SEM. *P < 0.05, **P < 0.01, ***P < 0.001.

3.6. PFOA inhibits the angiogenesis by reducing the nucleus accumulation of β-catenin in HUVECs

The Wnt/β-catenin signaling pathway is known to regulate angiogenesis [29–31]. When the canonical Wnt pathway is activated, GSK-3β is phosphorylated at Ser9 and thereby inactivated, leading to dissociation of the cytoplasmic β-catenin destruction complex and subsequent suppression of β-catenin ubiquitination and degradation. Then, β-catenin translocates into the nucleus, where it acts as a transcriptional activator in collaboration with lymphoid enhancer factor/T-cell factor (LEF/TCF) to regulate target gene expression [32]. Based on our finding that PFOA inhibited the GSK-3β phosphorylation, we speculated that PFOA suppressed the nuclear translocation of β-catenin. Immunofluorescence analysis showed that β-catenin was predominantly located in the cytoplasm in HUVECs after PFOA treatment, suggesting that PFOA induced cytoplasmic retention of β-catenin (Figure 7A).

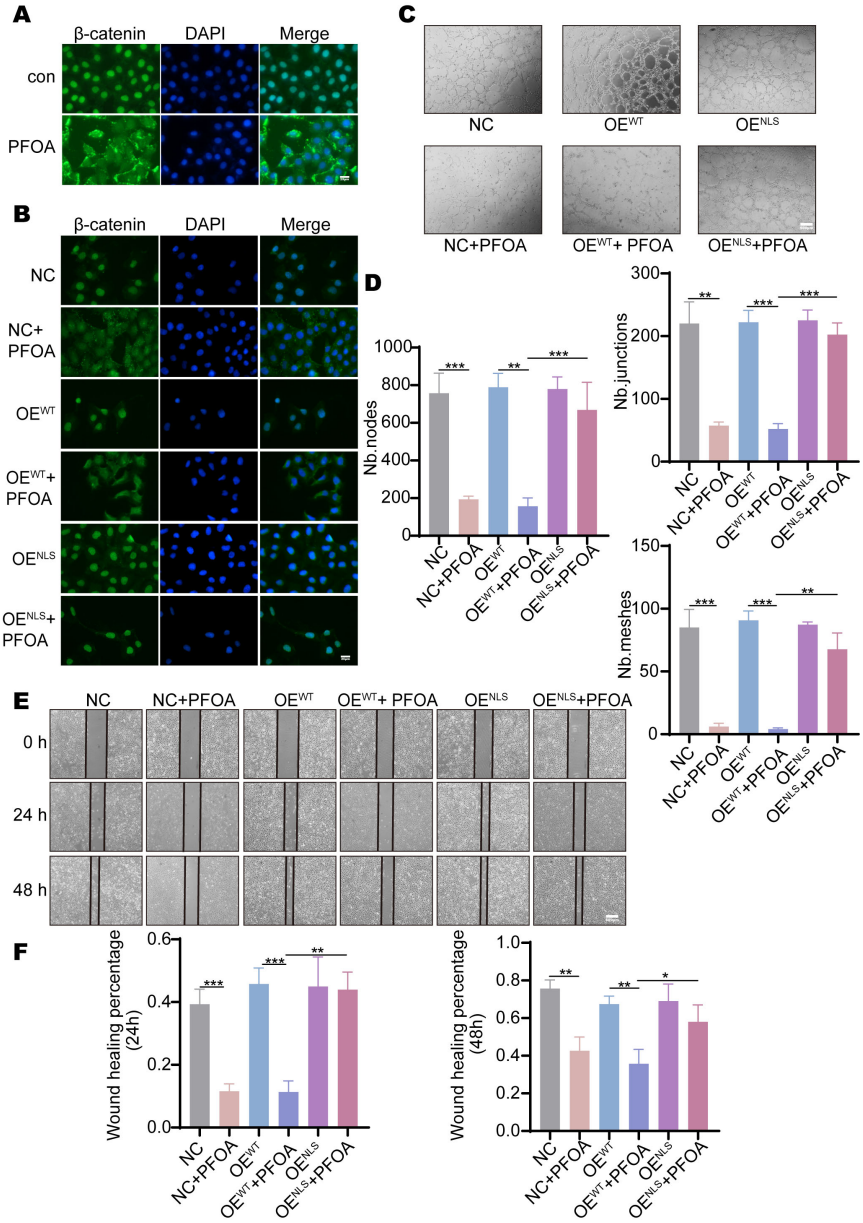


Figure 7. Effects of nuclear localization of β-catenin on angiogenesis in HUVECs treated with PFOA. **(A)** Immunostaining of β-catenin subcellular localization in HUVECs treated with PFOA. Bars indicate 25 μm; **(B)** Immunostaining of β-catenin subcellular localization in HUVECs overexpressing wild-type β-catenin (OE-β-catenin WT) and nuclear localization signal (NLS)-fused β-catenin (OE-β-catenin NLS) treated with PFOA. Bars indicate 25 μm; **(C, D)** In the tube formation assay, OE-β-catenin WT and OE-β-catenin NLS were treated with PFOA (40 μM), or not, for 24 hours and photographed after 3 hours (n = 3). Bars indicate 500 μm; **(E, F)** In the scratch assay, OE-β-catenin WT and OE-β-catenin NLS were treated with PFOA (40 μM), or not, and photographed at 0, 24, and 48 hours (n = 3). Bars indicate 500 μm. Data are represented as the mean ± SEM. *P < 0.05, **P < 0.01, ***P < 0.001.

To investigate whether the localization of β-catenin is responsible for PFOA inhibition of angiogenesis, we constructed plasmids overexpressing wild-type β-catenin (OE-β-catenin ^{WT}) and nuclear localization signal (NLS)-fused β-catenin (OE-β-catenin ^{NLS}). We transfected the OE-β-catenin ^{NLS} plasmid into HUVECs to obtain cells with stable nuclear expression of β-catenin (green fluorescence). The β-catenin was successfully localized in the nucleus, and PFOA treatment did not induce the nuclear export of β-catenin in the OE-β-catenin ^{NLS} group (Figure 7B). Following PFOA treatment, the OE-β-catenin ^{NLS} group exhibited enhanced tube formation and cell migration relative to the OE-β-catenin ^{WT} group (Figure 7C–F). These findings suggest the nuclear localization of β-catenin was critical for HUVECs angiogenesis, and PFOA inhibited HUVECs angiogenesis by blocking nuclear translocation of β-catenin.

3.7. PFOA inhibits the angiogenesis via β-catenin/Snail signaling in HUVECs

Endothelial-to-mesenchymal transition (EndMT) has been implicated in endothelial dysfunction and cardiovascular disease [33,34]. To investigate whether the impaired

angiogenic function of HUVECs was accompanied by changes in endothelial/mesenchymal markers, we examined a panel of EndMT-associated markers. Western blotting and qPCR analysis showed that PFOA suppressed the transcription factor (Snail) and the endothelial marker VE-cadherin, while there was no significant change in the expression of the mesenchymal markers N-cadherin and vimentin (Figure 8A–C). These changes indicate a partial loss of endothelial marker expression rather than classical EndMT, which typically requires a bidirectional marker switch (loss of endothelial markers with concomitant gain of mesenchymal markers). Mechanistically, nuclear-translocated β-catenin forms a functional transcriptional complex with LEF/TCF transcription factors, which directly binds to the promoter region of the Snail gene and initiates Snail transcription. Reduced β-catenin nuclear accumulation triggered by GSK-3β hyperactivation therefore profoundly diminishes Snail expression, ultimately disrupting endothelial angiogenic function. Snail is a downstream target gene of β-catenin, and is transcriptionally regulated by it. We then explored whether PFOA-induced endothelial marker dysregulation could be reversed by nuclear localization of β-catenin in HUVECs. Western blot results demonstrated that Snail expression was restored in the OE-β-catenin ^{NLS} group following PFOA treatment, indicating that the PFOA-induced inhibition of Snail could be countered by nuclear localization of β-catenin (Figure 8D,E).

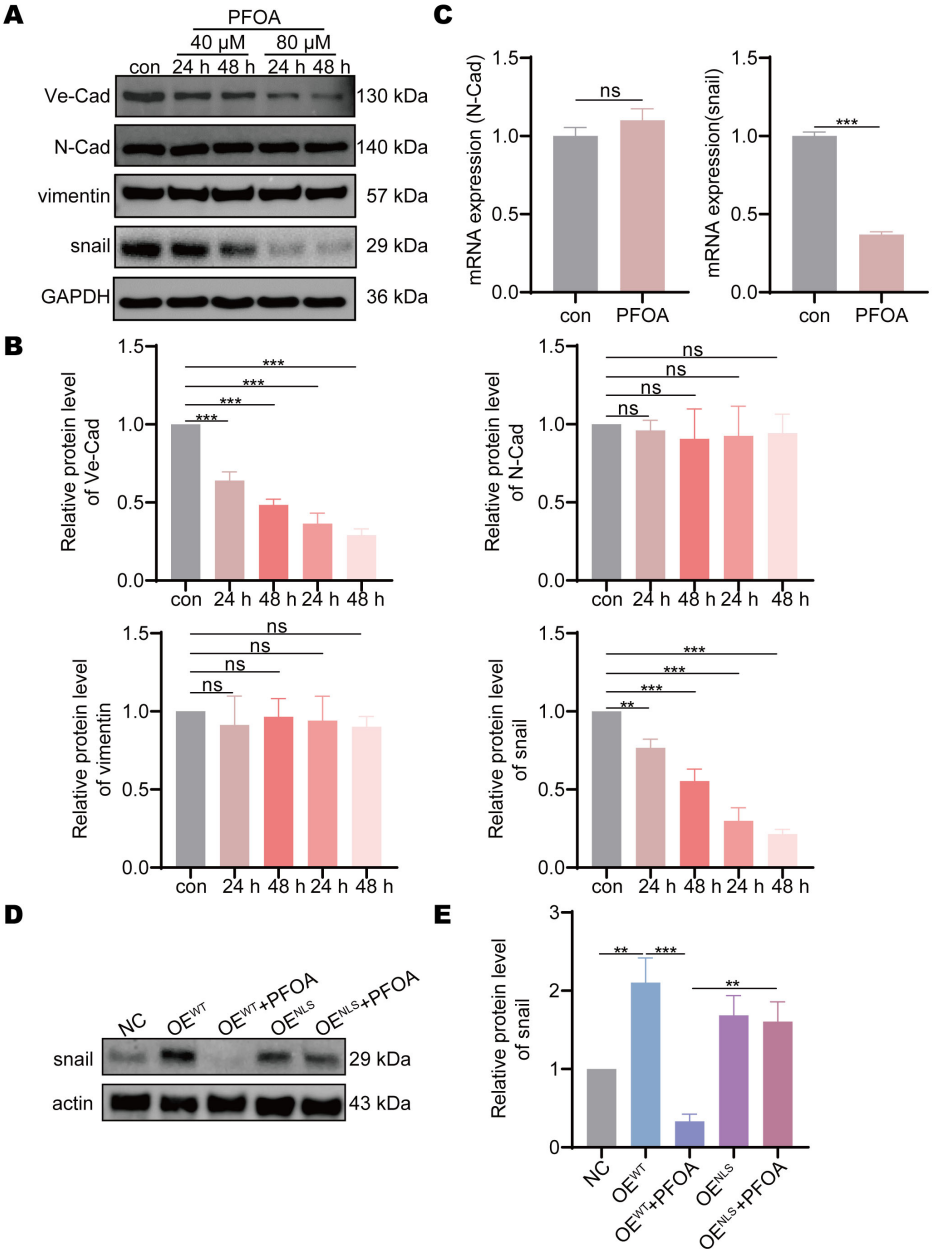


Figure 8. Effects of PFOA on endothelial marker expression in HUVECs. **(A, B)** The protein expression levels of endothelial and mesenchymal markers in HUVECs treated with PFOA were detected by western blot; **(C)** The mRNA expression levels of endothelial and mesenchymal markers in HUVECs treated with PFOA were detected by qPCR; **(D, E)** The protein expression level of Snail in NC, OE-β-catenin WT and OE-β-catenin NLS cells treated with PFOA or not was detected by western blot. Data are represented as the mean ± SEM. *P < 0.05, **P < 0.01, ***P < 0.001.

Finally, we overexpressed Snail in HUVECs (Figure 9A–C), and treated the cells with 40 μM PFOA for 24 hours. Tube formation and wound healing assays revealed that the angiogenic impairment caused by PFOA in HUVECs could be rescued by Snail overexpression (Figure 9D–G). These findings demonstrate that PFOA inhibits angiogenesis in HUVECs through the β-catenin/Snail signaling pathway.

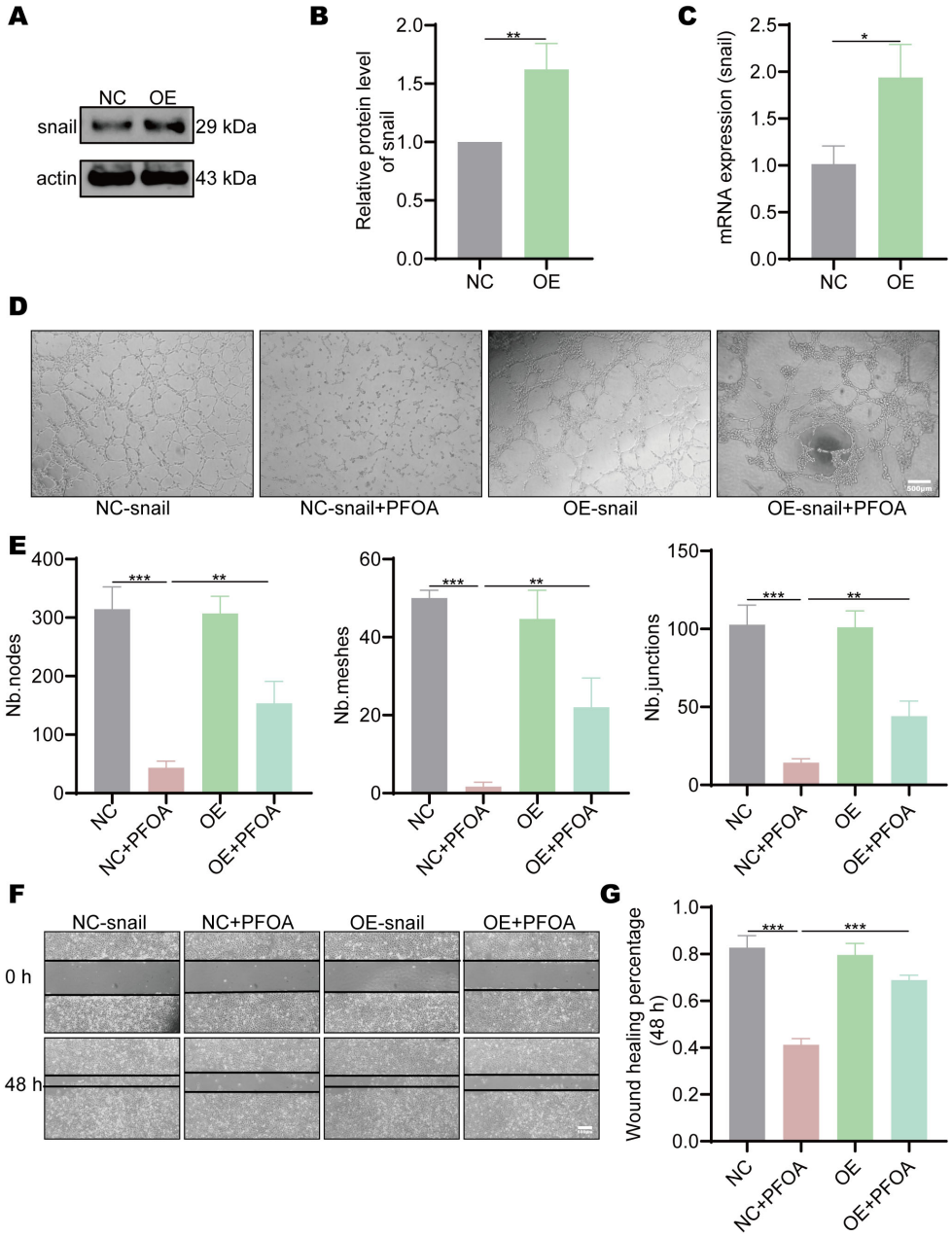


Figure 9. Effects of Snail on angiogenesis in HUVECs treated with PFOA. **(A, B)** The protein expression level of Snail in HUVECs infected with snail overexpressing and control lentivirus was detected by western blot; **(C)** The mRNA expression level of snail in HUVECs infected with snail overexpressing (OE) and control (NC) lentivirus was detected by qPCR; **(D, E)** In the tube formation assay, NC and OE group were treated with PFOA (40 μM), or not, for 24 hours and photographed after 3 hours (n = 3). Bars indicate 500 μm; **(F, G)** In the scratch assay, NC and OE group were treated with PFOA (40 μM), or not, and photographed at 0 and 48 hours (n = 3). Bars indicate 500 μm. Data are represented as the mean ± SEM. *P < 0.05, **P < 0.01, ***P < 0.001.

4. Discussion and conclusion

Given the worldwide distribution and extreme persistence of PFOA in the environment, concerns about its potential accumulation in the human body are increasing. Since cardiovascular diseases (CVDs) remain a major global health burden, interest in understanding the possible link between PFOA and CVDs is growing. Population-based cohort studies have demonstrated that chronic exposure to PFOA, as reflected by serum concentrations, is positively associated with an increased incidence of cardiovascular diseases, including hypertension,

hypercholesterolemia, and coronary artery disease [35,36]. However, the effects of PFOA on angiogenesis, especially in endothelial cells, remain poorly understood. In this study, we demonstrated that PFOA caused arterial intimal damage and inhibited angiogenesis in both *in vivo* and *in vitro* models. High concentrations of PFOA were found to reduce the viability, migration, and tube formation of HUVECs. Specifically, PFOA impaired angiogenesis of HUVECs by disrupting the PKA/GSK-3β/β-catenin/Snail signaling cascade. Our study suggests that PFOA-induced endothelial dysfunction may contribute to its cardiotoxic effects, filling a gap in understanding PFOA-induced cardiotoxicity. This novel mechanism could provide a strategy to mitigate exposure to this environmental contaminant.

Factors, such as inflammation, oxidative stress, hyperglycemia, hypoxia and toxins, play significant roles in damaging endothelial function and contributing to disease [37]. In our *in vitro* and *in vivo* experiments, we observed substantial endothelial dysfunction and vascular injury, including aortic intimal thickening, disorganized cells, and increased levels of inflammatory and oxidative stress markers, indicating that PFOA induces aortic intimal damage. Since high concentrations of PFOA were mainly linked with developmental cardiotoxicity in zebrafish and chicken models [18–20,38], studies on vascular injury and endothelial dysfunction were limited. Some animal experiments have shown that PFOS can cause heart and vascular morphological changes, such as cardiac hypertrophy, aortic intimal thickening, and significant increases in inflammation and oxidative stress [39,40]. Our findings are consistent with previous results and provide evidence that PFOA induces aortic intimal damage. Notably, the most prominent *in vivo* changes induced by PFOA were vascular inflammation and oxidative stress, which are themselves well-established suppressors of PKA activity. This raises the possibility that the PKA inhibition observed *in vitro* may be triggered not only directly by PFOA, but also secondarily by oxidative stress and inflammatory mediators—a possibility that we discuss below in the context of our mechanistic findings.

Endothelial dysfunction, characterized by hyperproliferation, angiogenic disorder, and endothelial-to-mesenchymal transition, is considered the pathophysiological basis of CVDs, including peripheral vascular diseases, atherosclerosis, stroke, and hypertension [11,41]. We found that PFOA caused dose-dependent inhibition of HUVEC viability, in accordance with previous studies. A high concentration of PFOA treatment in HUVECs suppressed tube formation and migration, indicating inhibition of angiogenesis. Additionally, several environmental toxins have been reported to lead to endothelial dysfunction, such as arsenic trioxide, bisphenol A and mercury [42].

Notably, the exposure concentrations and regimens adopted in our *in vivo* and *in vitro* experiments exhibit inherent differences from routine human environmental exposure, which affects the generalizability of research conclusions. In this study, the *in vivo* mouse model utilized 5 mg/L PFOA drinking water exposure for 9 weeks, which was designed to simulate the serum PFOA levels of highly exposed occupational populations (1.3–12.9 μg/mL), rather than general environmental exposure. For *in vitro* cellular experiments, we adopted a concentration gradient of 0–400 μM PFOA, with a subcytotoxic concentration of 40 μM selected for mechanistic exploration, and these *in vitro* concentrations are substantially higher than the serum PFOA levels observed in the general human population. Such discrepancies stem from fundamental differences between *in vitro* and *in vivo* exposure systems: HUVECs receive continuous, direct PFOA exposure without systemic metabolism, excretion, or tissue barrier isolation, leading to sustained intracellular PFOA accumulation, whereas human *in vivo* exposure is intermittent and modulated by metabolic clearance and blood-tissue barriers. Despite the concentration gap, high-concentration *in vitro* treatment is a standard strategy for precise mechanistic exploration by eliminating complex systemic interference, and our occupationally relevant *in vivo* exposure validates the biological plausibility of PFOA-induced vascular injury.

To investigate how PFOA exposure inhibits angiogenesis in HUVECs, we performed RNA sequencing analysis on HUVECs treated with PFOA. We identified 463 differentially expressed genes (DEGs), and functional enrichment analysis showed that these DEGs were significantly enriched in the PKA signaling pathway. cAMP activates PKA by binding to its regulatory subunit, leading to the release of the catalytic subunit, which then phosphorylates serine/threonine residues on target proteins to regulate cellular functions [43]. PKA increases the binding affinity of VEGFR2 to VEGF by phosphorylation of VEGFR2 [44], promoting VEGF signal transmission and activating downstream pathways such as PI3K/Akt and Ras/MAPK, which are vital for the proliferation, migration, and survival of vascular endothelial cells, key steps in angiogenesis [45]. Additionally, PKA can phosphorylate HIF-1α, a transcription factor controlling VEGF expression, thus upregulating VEGF and indirectly supporting angiogenesis [46,47]. Furthermore, PKA phosphorylates cytoskeletal proteins, including actin-binding proteins, thereby regulating cytoskeletal reorganization. This allows endothelial cells to migrate more efficiently, fostering the formation of new vascular sprouts and networks during angiogenesis [48,49]. Our experimental results showed that stimulation with 8-BA, a PKA activator, increased p-PKA levels in HUVECs and rescued the anti-angiogenic effect. These findings not only reinforce that PKA activity is required for normal

angiogenesis, but also highlight the harmful impacts of PFOA on endothelial cell function.

Taken together, our *in vivo* observations (induction of inflammatory cytokines and oxidative stress) and *in vitro* findings (suppression of PKA phosphorylation) raise an important question: does PFOA inhibit PKA directly, or indirectly through oxidative stress and inflammatory signaling? Both routes are biologically plausible. On the one hand, reactive oxygen species can directly oxidize cysteine residues in the activation loop of the PKA catalytic subunit, impairing its activity [50]; on the other hand, TNF-α stimulates cellular ceramide generation, and ceramide can activate protein phosphatase 2A (PP2A) [51], which may dephosphorylate and inactivate PKA. In addition, PFAS exposure—including PFOS—has been shown to induce ROS production in endothelial cells [52,53], so even in the HUVEC monoculture system, oxidative stress may contribute to the observed reduction in p-PKA.

We wish to emphasize that the primary aim of the present study was to identify the executing pathway downstream of PKA inhibition (the GSK-3β/β-catenin/Snail cascade and its functional consequences), rather than to dissect the upstream trigger. The observation that pharmacological activation of PKA by 8-BA substantially rescued PFOA-induced angiogenic defects indicates that suppression of PKA activity is a critical, required node in this process, irrespective of whether PKA inhibition is initiated directly or via oxidative stress/inflammatory mediators. Dissecting the relative contribution of direct versus indirect PKA inhibition—for example, using antioxidants such as *N*-acetylcysteine or PP2A inhibitors—warrants future investigation.

To explore the potential downstream regulatory targets of PKA, we focused on the GSK-3β, YAP, and PDK1 signaling pathways. Our study suggested that PFOA, by inhibiting PKA, attenuates the inhibitory phosphorylation of GSK-3β at Ser9, leading to GSK-3β activation. PKA activation leads to the phosphorylation of GSK-3β, which inhibits its activity and prevents the phosphorylation and degradation of β-catenin, promoting its translocation to the nucleus [54]. The immunofluorescence analysis confirmed that PFOA treatment resulted in the cytoplasmic retention of β-catenin in HUVECs, which is a key mechanism underlying the inhibition of angiogenesis. This inhibition of β-catenin nuclear translocation impaired angiogenesis under PFOA exposure. Notably, overexpression of wild-type or nuclear-localized β-catenin did not further enhance angiogenesis under basal conditions, likely because endogenous Wnt/β-catenin signaling in HUVECs cultured under optimized angiogenic conditions is already sufficient; however, nuclear-localized β-catenin specifically preserved angiogenic capacity under PFOA stress. This indicates that maintaining nuclear β-catenin is critical for resistance to PFOA-induced injury, rather than for enhancing angiogenesis per se. Decreased GSK-3β activity or hyperactive Wnt signaling induces β-catenin accumulation and nuclear translocation, triggering oncogene expression and promoting tumor cell proliferation, invasion, and metastasis [55]. The Wnt/β-catenin signaling pathway is known to play a role in endothelial cell proliferation and migration by regulating cytoskeletal proteins and promoting VEGF secretion, which is critical for angiogenesis [32,56]. These findings indicated the role of the PKA/GSK-3β/β-catenin signaling axis in PFOA-induced endothelial dysfunction.

PFOA exposure reduced the expression of the endothelial marker VE-cadherin and the transcription factor Snail, without significantly altering the mesenchymal markers N-cadherin and vimentin (Figure 8), indicating a partial loss of endothelial identity rather than classical endothelial-to-mesenchymal transition (EndMT), a process that contributes to vascular dysfunction and fibrosis [57]. Snail is a central inducer of epithelial–mesenchymal transition (EMT): it promotes the loss of cell polarity and intercellular junctions by suppressing epithelial markers such as E-cadherin [58] and its activity is augmented by Wnt/β-catenin signaling, which drives β-catenin nuclear translocation and thereby enhances cell migration and invasion [59,60]. In line with these roles, our findings suggest that PFOA-induced reduction of Snail expression, together with the suppression of β-catenin nuclear translocation, contributes to impaired angiogenesis. Consistently, overexpression of Snail restored tube formation and migration, effectively rescuing the angiogenic defects caused by PFOA exposure. These findings underscore the significance of Snail in regulating endothelial function and highlight its potential as a therapeutic target against PFOA-induced angiogenic dysfunction.

Collectively, this study establishes a complete and hierarchical PKA/GSK-3β/β-catenin/Snail regulatory network to interpret PFOA-mediated endothelial angiogenic dysfunction. Mechanistically, PFOA-induced PKA suppression serves as the core upstream event, which relieves GSK-3β from Ser9 inhibitory phosphorylation and sustains constitutive GSK-3β activation. Hyperactive GSK-3β continuously triggers cytoplasmic β-catenin degradation, blocks β-catenin nuclear translocation, and consequently restricts LEF/TCF-mediated transcriptional activation of Snail. The downregulation of Snail further reduces endothelial angiogenic capacity and partially impairs endothelial identity, ultimately contributing to vascular intimal injury and anti-angiogenic phenotypes. This integrated mechanistic cascade clarifies the sequential molecular events linking PFOA exposure to endothelial dysfunction and resolves the previously unclear transition from GSK-3β modulation to downstream β-catenin/Snail signaling alteration.

Nevertheless, this study has several unavoidable limitations. First, we used only a single cell line (HUVECs), and the results have not been validated in other vascular

endothelial cell subtypes. Second, the *in vitro* high-concentration and continuous PFOA treatment cannot fully replicate the low-dose, long-term intermittent exposure characteristics of general human populations, which limits the direct generalization of our quantitative concentration-effect results to ordinary environmental exposure scenarios. Third, the present study did not experimentally dissect whether PKA inhibition is triggered directly by PFOA or secondarily via oxidative stress and inflammatory signaling. In addition, the PKA activator 8-BA was used at a relatively high concentration (1 mM), which may induce potential off-target effects. Furthermore, the pharmacological rescue experiments with 8-BA and LiCl did not set up standalone drug-only and vehicle control groups, which makes it difficult to completely exclude the potential influences of these pharmacological agents and solvent vehicles on the basal angiogenic capacity of endothelial cells. Although consistent rescue phenotypes observed in both pharmacological intervention and genetic overexpression experiments strongly support the regulatory role of the PKA/GSK-3β/β-catenin/Snail axis in PFOA-induced angiogenic dysfunction, follow-up studies will supplement these blank control groups to further distinguish the baseline effects of intervention reagents from the specific rescue effects against PFOA toxicity. Future studies will adopt low-dose long-term exposure models combined with multiple endothelial cell lines and human tissue samples to further verify the translational applicability of the proposed toxicological mechanism and optimize the exposure dose-response relationship. In addition, different internal reference proteins (GAPDH and β-actin) were used for Western blot loading controls in different experimental batches, which represents a limitation of this study.

In summary, our study provided novel insights into the mechanisms by which PFOA impairs angiogenesis in endothelial cells. We found that PFOA exposure inhibits PKA phosphorylation and reduces the inhibitory phosphorylation of GSK-3β at Ser9, leading to the accumulation of β-catenin in the cytoplasm and decreased Snail expression. These events disrupt endothelial cell proliferation, migration, and tube formation, ultimately impairing angiogenesis. Our findings suggest that the anti-angiogenic effects of PFOA may contribute to its cardiotoxicity, providing a potential strategy for future therapeutic development. This study also emphasizes the importance of understanding the vascular effects of environmental contaminants on cardiovascular health.

Data availability statement

No supplementary or additional data were generated in this study.

Declaration of generative AI and AI-assisted technologies

The authors did not use generative AI or AI-assisted technologies in the writing of this manuscript.

Acknowledgments

Funding: This study was funded by Department of Science and Technology of Liaoning Province (2024JH2/102600320, 2024010054-JH3/101, 2024010428-JH3/107), and Shenyang Municipal Bureau of Science and Technology (22–321–31–03). The authors thank Haiyan Zhang and Xin Meng for their supervision and resources, Yixuan Liu for validation, methodology, investigation, data curation and conceptualization, and Dantong Lv for software and methodology.

Authors' contribution

Conceptualization, H.X. and Y.L.; methodology, H.X., Y.L. and D.L.; software, H.X. and D.L.; validation, H.X. and Y.L.; formal analysis, H.X.; investigation, Y.L.; resources, H.Z. and X.M.; data curation, Y.L.; writing—original draft preparation, H.X.; writing—review and editing, L.Y., L.Z., W.Z. and M.A.; visualization, H.X.; supervision, H.Z. and X.M.; project administration, H.Z.; funding acquisition, H.Z. All authors have read and agreed to the published version of the manuscript.

Conflicts of interest

The authors declare no conflicts of interest.

Ethical statement

All animal protocols were in accordance with the Guide for the Care and Use of Laboratory Animals (National Research Council) and were approved by the Institutional Animal Care and Use Committee (IACUC) of OBIO Biotechnology (Shanghai) Co., Ltd (Approval No. 166, Approval Date: July 12, 2022).

References

[1] Dhore R, Murthy GS. Per/polyfluoroalkyl substances production, applications and environmental impacts. *Bioresour. Technol.* 2021, 341:125808. DOI: 10.1016/j.biortech.2021.125808

[2] Panieri E, Baralic K, Djukic-Cosic D, Buha Djordjevic A, Saso L. PFAS molecules: a major concern for the human health and the environment. *Toxics* 2022, 10(2):44. DOI: 10.3390/toxics10020044

[3] Cousins IT, DeWitt JC, Gluge J, Goldenman G, Herzke D, *et al.* Strategies for grouping per- and polyfluoroalkyl substances (PFAS) to protect human and environmental health. *Environ. Sci.: Processes Impacts* 2020, 22(7):1444–1460. DOI: 10.1039/d0em00147c

[4] Lohmann R, Letcher RJ. The universe of fluorinated polymers and polymeric substances and potential environmental impacts and concerns. *Curr. Opin. Green Sustain. Chem.* 2023, 41:100795. DOI: 10.1016/j.cogsc.2023.100795

[5] Zong S, Wang L, Wang S, Wang Y, Jiang Y, *et al.* Exposure to per- and polyfluoroalkyl substances is associated with impaired cardiovascular health: a cross-sectional study. *Front. Public Health* 2024, 12:1418134. DOI: 10.3389/fpubh.2024.1418134

[6] Batzella E, Rosato I, Pitter G, Da Re F, Russo F, *et al.* Determinants of PFOA serum half-life after end of exposure: a longitudinal study on highly exposed subjects in the Veneto region. *Environ. Health Perspect.* 2024, 132(2):027002. DOI: 10.1289/EHP13152

[7] Zhang Z, Sarkar D, Biswas JK, Datta R. Biodegradation of per- and polyfluoroalkyl substances (PFAS): a review. *Bioresour. Technol.* 2022, 344:126223. DOI: 10.1016/j.biortech.2021.126223

[8] Rosato I, Bonato T, Fletcher T, Batzella E, Canova C. Estimation of per- and polyfluoroalkyl substances (PFAS) half-lives in human studies: a systematic review and meta-analysis. *Environ. Res.* 2024, 242:117743. DOI: 10.1016/j.envres.2023.117743

[9] Barton KE, Zell-Baran LM, DeWitt JC, Brindley S, McDonough CA, *et al.* Cross-sectional associations between serum PFASs and inflammatory biomarkers in a population exposed to AFFF-contaminated drinking water. *Int. J. Hyg. Environ. Health* 2022, 240:113905. DOI: 10.1016/j.ijheh.2021.113905

[10] Xu D, Li L, Tang L, Guo M, Yang J. Perfluorooctane sulfonate induces heart toxicity involving cardiac apoptosis and inflammation in rats. *Exp. Ther. Med.* 2022, 23(1):14. DOI: 10.3892/etm.2021.10936

[11] Wen Z, Wei Y, Zhang Y, Zhang Y. A review of cardiovascular effects and underlying mechanisms of legacy and emerging per- and polyfluoroalkyl substances (PFAS). *Arch. Toxicol.* 2023, 97(5):1195–1245. DOI: 10.1007/s00204-023-03477-5

[12] Wang Y, Jiang S, Wang B, Chen X, Lu G. Comparison of developmental toxicity induced by PFOA, HFPO-DA, and HFPO-TA in zebrafish embryos. *Chemosphere* 2023, 311:136999. DOI: 10.1016/j.chemosphere.2022.136999
[13] Wasel O, Thompson KM, Freeman JL. Assessment of unique behavioral, morphological, and molecular alterations in the comparative developmental toxicity profiles of PFOA, PFHxA, and PFBA using the zebrafish model system. *Environ. Int.* 2022, 170:107642. DOI: 10.1016/j.envint.2022.107642
[14] Schlezinger JJ, Gokce N. Perfluoroalkyl/polyfluoroalkyl substances: links to cardiovascular disease risk. *Circ. Res.* 2024, 134(9):1136–1159. DOI: 10.1161/circresaha.124.323697
[15] Boafo YS, Mostafa S, Obeng-Gyasi E. Association of combined metals and PFAS with cardiovascular disease risk. *Toxics* 2023, 11(12):979. DOI: 10.3390/toxics11120979
[16] Wee SY, Aris AZ. Environmental impacts, exposure pathways, and health effects of PFOA and PFOS. *Ecotoxicol. Environ. Saf.* 2023, 267:115663. DOI: 10.1016/j.ecoenv.2023.115663
[17] Yu J, Cheng W, Jia M, Chen L, Gu C, *et al.* Toxicity of perfluorooctanoic acid on zebrafish early embryonic development determined by single-cell RNA sequencing. *J. Hazard. Mater.* 2022, 427:127888. DOI: 10.1016/j.jhazmat.2021.127888
[18] Li J, Hu C, Zhao B, Li J, Chen L. Proteomic and cardiac dysregulation by representative perfluoroalkyl acids of different chemical speciation during early embryogenesis of zebrafish. *Sci. Total Environ.* 2024, 926:172000. DOI: 10.1016/j.scitotenv.2024.172000
[19] Ni H, Yuan J, Ji J, Guo Y, Zhong S, *et al.* Long term toxicities following developmental exposure to perfluorooctanoic acid: roles of peroxisome proliferation activated receptor α. *Environ. Pollut.* 2023, 317:120722. DOI: 10.1016/j.envpol.2022.120722
[20] Liu X, Chen R, Peng Y, Zhou Y, Xia M, *et al.* Perfluorooctanoic acid (PFOA) induces cardiotoxicity by activating the Keap1/Nrf2 pathway in zebrafish (*Danio rerio*) embryos. *Ecotoxicol. Environ. Saf.* 2024, 285:117098. DOI: 10.1016/j.ecoenv.2024.117098
[21] Guerra A, Belinha J, Mangir N, MacNeil S, Natal Jorge R. Simulation of the process of angiogenesis: quantification and assessment of vascular patterning in the chicken chorioallantoic membrane. *Comput. Biol. Med.* 2021, 136:104647. DOI: 10.1016/j.compbiomed.2021.104647
[22] Chen J, Liang X, Zhang S, Wang S, Garcia SP, *et al.* Two faces of bivalent domain regulate VEGFA responsiveness and angiogenesis. *Cell Death Dis.* 2020, 11(1):75. DOI: 10.1038/s41419-020-2228-3
[23] Hasan SS, Fischer A. Notch signaling in the vasculature: angiogenesis and angiocrine functions. *Cold Spring Harb. Perspect. Med.* 2023, 13(2):a041166. DOI: 10.1101/cshperspect.a041166
[24] Omorphos NP, Gao C, Tan SS, Sangha MS. Understanding angiogenesis and the role of angiogenic growth factors in the vascularisation of engineered tissues. *Mol. Biol. Rep.* 2021, 48(1):941–950. DOI: 10.1007/s11033-020-06108-9
[25] Costa G, Sartori S, Consonni D. Thirty years of medical surveillance in perfluorooctanoic acid production workers. *J. Occup. Environ. Med.* 2009, 51(3):364–372. DOI: 10.1097/jom.0b013e3181965d80
[26] Sakr CJ, Leonard RC, Kreckmann KH, Slade MD, Cullen MR. Longitudinal study of serum lipids and liver enzymes in workers with occupational exposure to ammonium perfluorooctanoate. *J. Occup. Environ. Med.* 2007, 49(8):872–879. DOI: 10.1097/jom.0b013e318124a93f
[27] Huang DW, Sherman BT, Lempicki RA. Systematic and integrative analysis of large gene lists using DAVID bioinformatics resources. *Nat. Protoc.* 2009, 4(1):44–57. DOI: 10.1038/nprot.2008.211
[28] Tiruppathi C, Malik AB, Del Vecchio PJ, Keese CR, Giaever I. Electrical method for detection of endothelial cell shape change in real time: assessment of endothelial barrier function. *Proc. Natl. Acad. Sci. U.S.A.* 1992, 89(17):7919–7923. DOI: 10.1073/pnas.89.17.7919
[29] Fu W, Wang W, Zeng C. Wnt signaling pathways in myocardial infarction and the therapeutic effects of Wnt pathway inhibitors. *Acta Pharmacol. Sin.* 2019, 40(1):9–12. DOI: 10.1038/s41401-018-0060-4
[30] Jiang L, Yin M, Wei X, Liu J, Wang X, *et al.* Bach1 represses Wnt/β-catenin signaling and angiogenesis. *Circ. Res.* 2015, 117(4):364–375. DOI: 10.1161/CIRCRESAHA.115.306829
[31] Zhang Q, Wang L, Wang S, Cheng H, Xu L, *et al.* Signaling pathways and targeted therapy for myocardial infarction. *Signal Transduct. Target. Ther.* 2022, 7(1):78. DOI: 10.1038/s41392-022-00925-z
[32] Yang F, Guo J, Kang N, Yu X, Ma Y. rESWT promoted angiogenesis via Bach1/Wnt/β-catenin signaling pathway. *Sci. Rep.* 2024, 14(1):11733. DOI: 10.1038/s41598-024-62582-2
[33] Souilhol C, Harmsen MC, Evans PC, Krenning G. Endothelial-mesenchymal transition in atherosclerosis. *Cardiovasc. Res.* 2018, 114(4):565–577. DOI: 10.1093/cvr/cvx253
[34] Alvandi Z, Bischoff J. Endothelial-mesenchymal transition in cardiovascular disease. *Arterioscler. Thromb. Vasc. Biol.* 2021, 41(9):2357–2369. DOI: 10.1161/atvbaha.121.313788
[35] Liao S, Yao W, Cheang I, Tang X, Yin T, *et al.* Association between perfluoroalkyl acids and the prevalence of hypertension among US adults. *Ecotoxicol. Environ. Saf.* 2020, 196:110589. DOI: 10.1016/j.ecoenv.2020.110589
[36] Winquist A, Steenland K. Modeled PFOA exposure and coronary artery disease, hypertension, and high cholesterol in community and worker cohorts. *Environ. Health Perspect.* 2014, 122(12):1299–1305. DOI: 10.1289/ehp.1307943
[37] Grego A, Fernandes C, Fonseca I, Dias-Neto M, Costa R, *et al.* Endothelial dysfunction in cardiovascular diseases: mechanisms and *in vitro* models. *Mol. Cell. Biochem.* 2025, 480(8):4671–4695. DOI: 10.1007/s11010-025-05289-w
[38] Dangudubiyyam SV, Mishra JS, Song R, Kumar S. Maternal perfluorooctane sulfonic acid exposure during rat pregnancy causes hypersensitivity to angiotensin II and attenuation of endothelium-dependent vasodilation in the uterine arteries. *Biol. Reprod.* 2022, 107(4):1072–1083. DOI: 10.1093/biolre/ioac141
[39] Deng P, Wang C, Wahlang B, Sexton T, Morris AJ, *et al.* Co-exposure to PCB126 and PFOS increases biomarkers associated with cardiovascular disease risk and liver injury in mice. *Toxicol. Appl. Pharmacol.* 2020, 409:115301. DOI: 10.1016/j.taap.2020.115301
[40] Yu Y, Wang C, Zhang X, Zhu J, Wang L, *et al.* Perfluorooctane sulfonate disrupts the blood brain barrier through the crosstalk between endothelial cells and astrocytes in mice. *Environ. Pollut.* 2020, 256:113429. DOI: 10.1016/j.envpol.2019.113429
[41] Pasut A, Lama E, Van Craenenbroeck AH, Kroon J, Carmeliet P. Endothelial cell metabolism in cardiovascular physiology and disease. *Nat. Rev. Cardiol.* 2025, 22(12):923–943. DOI: 10.1038/s41569-025-01162-x
[42] Lamas GA, Bhatnagar A, Jones MR, Mann KK, Nasir K, *et al.* Contaminant metals as cardiovascular risk factors: a scientific statement from the American Heart Association. *J. Am. Heart Assoc.* 2023, 12(13):e029852. DOI: 10.1161/JAHA.123.029852
[43] Conca F, Bayburtlu DK, Vismara M, Surdo NC, Tavoni A, *et al.* Phosphatases control the duration and range of cAMP/PKA microdomains. *Function* 2025, 6(2):zqaf007. DOI: 10.1093/function/zqaf007
[44] Mariotti V, Fiorotto R, Cadamuro M, Fabris L, Strazzabosco M. New insights on the role of vascular endothelial growth factor in biliary pathophysiology. *JHEP Rep.* 2021, 3(3):100251. DOI: 10.1016/j.jhepr.2021.100251
[45] Kim T, Kang JK, Hyun CG. 6-Methylcoumarin promotes melanogenesis through the PKA/CREB, MAPK, AKT/PI3K, and GSK3β/β-catenin signaling pathways. *Molecules* 2023, 28(11):4551. DOI: 10.3390/molecules28114551
[46] Song S, Zhang G, Chen X, Zheng J, Liu X, *et al.* HIF-1α increases the osteogenic capacity of ADSCs by coupling angiogenesis and osteogenesis via the HIF-1α/VEGF/AKT/mTOR signaling pathway. *J. Nanobiotechnol.* 2023, 21(1):257. DOI: 10.1186/s12951-023-02020-z
[47] Liang H, Yin G, Shi G, Liu Z, Liu X, *et al.* Echinacoside regulates PI3K/AKT/HIF-1alpha/VEGF cross signaling axis in proliferation and apoptosis of breast cancer. *Anal. Biochem.* 2024, 684:115360. DOI: 10.1016/j.ab.2023.115360
[48] Beal R, Alonso-Carriazo Fernandez A, Grammatopoulos DK, Matter K, Balda MS. ARHGEF18/p114RhoGEF coordinates PKA/CREB signaling and actomyosin remodeling to promote trophoblast cell-cell fusion during placenta morphogenesis. *Front. Cell Dev. Biol.* 2021, 9:658006. DOI: 10.3389/fcell.2021.658006

[49] Halff EF, Hannan S, Kwanthongdee J, Lesept F, Smart TG, *et al.* Phosphorylation of neuroligin-2 by PKA regulates its cell surface abundance and synaptic stabilization. *Sci. Signal.* 2022, 15(739):eabg2505. DOI: 10.1126/scisignal.abg2505

[50] Humphries KM, Pennypacker JK, Taylor SS. Redox regulation of cAMP-dependent protein kinase signaling: kinase versus phosphatase inactivation. *J. Biol. Chem.* 2007, 282(30):22072–22079. DOI: 10.1074/jbc.m702582200

[51] Dobrowsky RT, Kamibayashi C, Mumby MC, Hannun YA. Ceramide activates heterotrimeric protein phosphatase 2A. *J. Biol. Chem.* 1993, 268(21):15523–15530. DOI: 10.1016/s0021-9258(18)82288-8

[52] Qian Y, Ducatman A, Ward R, Leonard S, Bukowski V, *et al.* Perfluorooctane sulfonate (PFOS) induces reactive oxygen species (ROS) production in human microvascular endothelial cells: role in endothelial permeability. *J. Toxicol. Environ. Health A* 2010, 73(12):819–836. DOI: 10.1080/15287391003689317

[53] Liao Y, Wang J, Huang QS, Fang C, Kiyama R, *et al.* Evaluation of cellular response to perfluorooctane sulfonate in human umbilical vein endothelial cells. *Toxicol. In Vitro* 2012, 26(3):421–428. DOI: 10.1016/j.tiv.2012.01.011

[54] Jahan S, Singh S, Srivastava A, Kumar V, Kumar D, *et al.* PKA-GSK3β and β-catenin signaling play a critical role in trans-resveratrol mediated neuronal differentiation in human cord blood stem cells. *Mol. Neurobiol.* 2018, 55(4):2828–2839. DOI: 10.1007/s12035-017-0539-x

[55] Wang Y, Hang K, Ying L, Wu J, Wu X, *et al.* LAMP2A regulates the balance of mesenchymal stem cell adipo-osteogenesis via the Wnt/β-catenin/GSK3β signaling pathway. *J. Mol. Med.* 2023, 101(7):783–799. DOI: 10.1007/s00109-023-02328-1

[56] Azhdari M, zur Hausen A. Wnt/β-catenin and notch signaling pathways in cardiovascular disease: mechanisms and therapeutics approaches. *Pharmacol. Res.* 2025, 211:107565. DOI: 10.1016/j.phrs.2024.107565

[57] Jiang H, Zhou Y, Zhang W, Li H, Ma W, *et al.* Molecular mechanisms of endothelial-mesenchymal transition and its pathophysiological feature in cerebrovascular disease. *Cell Biosci.* 2025, 15(1):49. DOI: 10.1186/s13578-025-01393-y

[58] Hosseini K, Trus P, Frenzel A, Werner C, Fischer-Friedrich E. Skin epithelial cells change their mechanics and proliferation upon snail-mediated EMT signalling. *Soft Matter* 2022, 18(13):2585–2596. DOI: 10.1039/d2sm00159d

[59] Anthony CC, Robbins DJ, Ahmed Y, Lee E. Nuclear regulation of Wnt/β-catenin signaling: it's a complex situation. *Genes* 2020, 11(8):886. DOI: 10.3390/genes11080886

[60] Lu X, Gong J, Dennery PA, Yao H. Endothelial-to-mesenchymal transition: pathogenesis and therapeutic targets for chronic pulmonary and vascular diseases. *Biochem. Pharmacol.* 2019, 168:100–107. DOI: 10.1016/j.bcp.2019.06.021